



## Executive summary

# Review of aeronautical fatigue investigations in the Netherlands during the period March 2007 - March 2009

**Report no.**

NLR-TP-2009-155

**Author(s)**

M.J. Bos

R.J.H. Wanhill

**Report classification**

UNCLASSIFIED

**Date**

May 2009

**Knowledge area(s)**Testen van vliegtuigconstructies  
en -materialenVliegtuigmateriaal- en  
schadeonderzoek

Vliegtuigmaterialen

Levensduurbewaking &amp;

Onderhoud van vliegtuigen

Lucht- en Ruimtevaart

Constructie- en

Fabricagetechnologie

**Descriptor(s)**

aerospace

aircraft

fatigue

ICAF

**Description of work**

This report is a review of the aerospace fatigue activities in the Netherlands during the period March 2007 to March 2009. The review is the Netherlands National

Delegate's contribution to the 31st Conference of the International Committee on Aeronautical Fatigue (ICAF), 25 and 26 May 2009, Rotterdam, the Netherlands.

This report has been prepared in the format required for presentation at the 31st Conference of the International Committee on Aeronautical Fatigue (ICAF), 25 and 26 May 2009, Rotterdam, the Netherlands.

**Review of aeronautical fatigue investigations in the Netherlands during the period March 2007 - March 2009**

**Nationaal Lucht- en Ruimtevaartlaboratorium**, National Aerospace Laboratory NLR

Anthony Fokkerweg 2, 1059 CM Amsterdam,  
P.O. Box 90502, 1006 BM Amsterdam, The Netherlands

Telephone +31 20 511 31 13, Fax +31 20 511 32 10, Web site: [www.nlr.nl](http://www.nlr.nl)



**provisional issue**

NLR-TP-2009-155

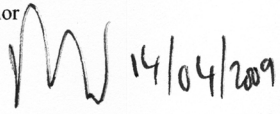
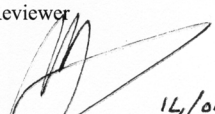
## **Review of aeronautical fatigue investigations in the Netherlands during the period March 2007 - March 2009**

M.J. Bos and R.J.H. Wanhill

This report has been prepared in the format required for presentation at the 31st Conference of the International Committee on Aeronautical Fatigue (ICAF), 25 and 26 May 2009, Rotterdam, the Netherlands.

Customer                      National Aerospace Laboratory NLR  
Contract number            -  
Owner                         National Aerospace Laboratory NLR  
Division NLR                 Aerospace Vehicles  
Distribution                 Beperkt  
Classification of title      Unclassified  
   May 2009

Approved by:

Author	Reviewer	Managing department
 14/04/2009	 14/04/2009	 14/4/09





## **Summary**

This report is a review of the aeronautical fatigue activities in the Netherlands during the period March 2007 to March 2009, and is the National Delegate's contribution to the 31<sup>st</sup> Conference of the International Committee on Aeronautical Fatigue (ICAF), 25 and 26 May 2009, Rotterdam, the Netherlands.



## Contents

1.1	INTRODUCTION .....	5
1.2	LOADS .....	5
1.3	STRUCTURAL LOADS/USAGE/HEALTH MONITORING.....	6
1.4	FIBRE/METAL LAMINATES (FMLs) FULL AND SUB-SCALE TESTS	11
1.5	FIBRE/METAL LAMINATES (FMLs) SPECIMEN TESTS .....	14
1.6	FATIGUE AND DAMAGE TOLERANCE STUDIES .....	16
1.7	FULL-SCALE AND DETAIL FATIGUE TESTING.....	19
1.8	SPECIAL CATEGORY .....	20
1.9	REFERENCES .....	21

## **Review of aeronautical fatigue investigations in the Netherlands during the period March 2007 – March 2009**

M.J. Bos and R.J.H. Wanhill  
National Aerospace Laboratory NLR  
Anthony Fokkerweg 2  
1006 BM Amsterdam  
The Netherlands

### **1.1 INTRODUCTION**

The present review gives a summary of the work performed in the Netherlands in the field of aerospace fatigue during the period from March 2007 to March 2009. The contributions to this review come from the following sources:

- The National Aerospace Laboratory NLR
- The Faculty of Aerospace Engineering, Delft University of Technology, TUD
- Stork Fokker AESP BV.

The names of the principal investigators and their affiliations are given at the end of the title for each topic.

### **1.2 LOADS**

#### **1.2.1 Computer aided sequencing of aircraft loads and stresses for fatigue analysis and testing, CLASS (R.P.G. Veul, NLR)**

The NLR has continued to develop the CLASS computer program. The CLASS program generates a sequence of loads or stresses automatically for an arbitrary aircraft structure, and was presented in the ICAF 2001 meeting. The CLASS program reduces the effort to generate flight-by-flight load and stress sequences for fatigue analysis and testing. CLASS has been used for aeroplanes (Airbus A380, A400M), for components (Airbus and Dassault movables), landing gears (F-16) and for helicopter parts (NH90 tail).

Class is operational at Stork Fokker AESP and at Airbus Germany and is currently being considered to become an all-Airbus preferred tool for the generation of spectra. A schematic of the CLASS program is given in figure 1. Two recent reports [1, 2] describe some of the ongoing developments and are summarised here:

(1) Coupling and enhancement of existing tools [1].

- Fast and efficient coupling of CLASS with the fatigue analysis tools SPRAC and FATDAC used by Stork Fokker AESP
- Development of sophisticated and user interactive CLASS input file generator ClinGUI and a concise user's manual
- Fast generation of complex load sequences with an updated version of CLASS.

Figure 2 shows the relations between the various tools.

- (2) Detection of fatigue-critical areas [2]. A plug-in for the FEM program PATRAN (see figure 2) was optimised to enable fatigue life predictions using the full load spectrum. The resulting enhanced tool for detecting fatigue-critical areas was verified for a real component, see figure 3. Use of this enhanced tool will improve the detection of problem areas during the early stages of design and help to avoid expensive changes at later stages.

### 1.3 STRUCTURAL LOADS/USAGE/HEALTH MONITORING

#### 1.3.1 Transport aircraft C-130H-30 Hercules: HOLMES (M.J. Bos, NLR)

The Royal Netherlands Air Force (RNLAf) C-130H-30 fleet is used in a much different way from that originally anticipated at the time of acquisition. Out-of-area operations, such as those performed under the ISAF flag in Afghanistan, severely stress the aircraft and adversely affect the airframe service life. The NLR has developed a loads and usage monitoring system called HOLMES (Hercules Operational Life Monitoring & Evaluation System) that brings together measured flight data and flight administrative data from various sources. The collected information is used to compute the expended fatigue life of critical areas of the airframe, e.g. figure 4. The RNLAf now employs this system as a tool to take informed decisions about fleet life management.

In principle, the underlying fatigue analysis method cannot be used to optimize the prescribed ASIP inspection intervals. This is because the method uses a Miner-type fatigue life approach rather than a non-linear method for fatigue crack growth prediction. The current method should therefore be regarded as a tool to determine the economic life for individual aircraft in the fleet. However, there are two upgrades in view:

- (1) In the near future the loads and usage monitoring programme will significantly benefit from retrofit of a “glass cockpit” associated with introduction of two additional C-130H aircraft to the RNLAf fleet. A study is currently being conducted to evaluate the new possibilities offered by the availability of the flight parameters on the MIL-1553 databus.
- (2) In 2009-2010 a measurement campaign will collect a set of loads data to enable the development damage rates based on fatigue crack growth. Initially this will be done for the centre wing only. At a later stage other structural areas will be surveyed on a “need-to” basis. The measurement campaign will use the NLR-developed stand-alone strain data acquisition system ‘SALSA’, see subsection 1.3.6.

#### 1.3.2 Helicopters: *HeliDamTol* (M.J. Bos, NLR)

The helicopter damage tolerance project HeliDamTol has two main objectives. The first is to develop reliable methods of fatigue crack growth analysis for helicopter airframe components. The second is to incorporate these methods into a demonstrator version of an Operational Damage Assessment Tool (ODAT) that can be used in operational circumstances or during line maintenance to assess the severity of any fatigue cracks found in the primary airframe structure. The ODAT should facilitate the decision whether or not to fly, and how to fly, with any damage that is present. In the case of out-of-area operations, the ODAT may be used to decide whether the required maintenance actions can be deferred to a more suitable time.

Figure 5 shows the ODAT system architecture. This reflects the overall procedure for calculating a safe fatigue crack growth life, i.e. the number of flight hours needed to grow the crack from its detected size to the size at which unstable fracture and failure occur. The overall procedure requires a reliable fatigue crack growth model and knowledge of the following parameters: (1) the local structural geometry and its impact on the crack driving force, (2) the type of material and the associated fatigue crack growth resistance, and (3) the expected loads environment:

- (1) Geomat / MatDat + K-fact / CraGro modules. For an existing crack the structural geometry and type of material at the crack location are obviously known. The impact of the local geometry on the crack driving force can be described with a stress intensity function obtainable from handbooks or finite element analyses. The material’s fatigue crack growth resistance can be derived from crack growth curves representing the growth rates,  $da/dN$ , as functions of the cyclic crack tip stress intensity,  $\Delta K$ , and the cyclic stress ratio  $R$ .

First estimates of crack growth rates can be obtained from handbooks, but in general additional testing is required to get accurate data. Within the HeliDamTol programme extensive experimental material data sets have been generated for materials pertinent to the RNLAf CH-47D “Chinook” and Royal Netherlands Navy (RNLN) NH90 helicopters. The required data have been obtained from the following types of tests:

- Fatigue crack growth thresholds
- Fatigue crack growth curves

- Cyclic stress-strain curves
- Monotonic true stress – true strain curves
- Simple spectrum fatigue crack growth
- Complex spectrum fatigue crack growth.

- (2) Mission / Spectrum modules. For the expected loads environment an artificial neural network-based tool (ANN) has been developed to correlate the local stress or strain response to the relevant flight parameters (e.g. IAS, altitude, etc.) and helicopter configuration. For the CH-47D these data are routinely collected with the CVFDR that has been installed fleetwide. Any desired mission profile can be assembled by selecting characteristic flights from the HELIUM database (also developed by the NLR). The associated local stress response sequence can then be used as input to the fatigue crack growth model.

A prerequisite for these activities is that one or more helicopters in the fleet are equipped with strain gauges and an additional data recorder. Strain data are first periodically collected at likely critical locations. Once a sufficient data set has been obtained to train the ANN for these locations, the strain gauges can be moved to other locations of interest. This eventually enables the entire airframe to be covered. This is already the case for the CH-47D fleet.

- (3) Spectrum / CraGro modules. For the final part of the procedure an accurate fatigue crack growth model has been developed that considers the local crack tip strain response to model the spectrum load interaction effects. The model is based on the so-called “Strip Yield” approach, which is considered to be state-of-the-art.

Validation of the various developed methods and tools and the overall procedure will be done in 2009.

### 1.3.3 Helicopters: Flight Regime Recognition (J.A.J.A. Dominicus, N. Munninghof, NLR)

The operational usage spectrum of a helicopter is generally expressed in terms of the percentage of time spent in the various pre-defined flight regimes and the number of occurrences of specific events such as ground-air-ground cycles, landings, etc. Consequently, the fatigue life consumption of critical helicopter components is usually monitored by tracking the accumulated time spent in each of these flight regimes and the cumulative number of occurrences of these events, and then combining this information with the OEM-specified (or otherwise obtained) fatigue damage rates for each critical component.

To facilitate this procedure it is highly desirable to have an automatic procedure for Flight Regime Recognition (FRR). The NLR has already developed such a procedure for the RNLAf CH-47D fleet. This procedure employs a physics-based algorithm that processes a number of the flight parameters that are available on the ARINC-429 databus. Recently this procedure has been tailored for application to the RNLAf AH-64D “Apache” helicopters, and a similar tool is currently being developed for the RNLN NH90 helicopters. Figure 6 illustrates the NH90 type.

### 1.3.4 Helicopters: CH-47D “Chinook” (A. Oldersma, NLR)

Strain gauge data are routinely collected within the framework of the RNLAf CH-47D “Chinook” loads and usage monitoring programme. For this purpose two airframes (the D-103, with machined frames, and the D-664, with built-up frames) have been equipped with an ACRA data acquisition unit and 9 strain gauges each, see figure 7. To enable detailed vibration analyses the strain gauge data were initially sampled at 1024 Hz, but later the sample rate was reduced to 512 Hz. This way it was possible to determine the contribution of specific frequencies like 1/rev, 2/rev, 3/rev etc. to the overall signal content. The contribution of vibration to the accumulation of fatigue damage was determined using rainflow counting and a linear damage (Miner’s) rule.

Besides strain gauge data, the data acquisition unit also records flight parameters. These flight parameters are the input for FRR (Flight Regime Recognition). The Flight Regime distribution, together with other usage statistics reveals differences in usage during out-of-area operations and usage in the Netherlands. The relative fatigue damage per flight regime was calculated using the associated strain gauge data.

The flight parameter dataset combined with strain gauge data offers the opportunity to zoom in on specific events or steady state flight conditions and determine the related relative fatigue damage. For example, the effect of parameters like air speed, altitude and aircraft weight on the relative fatigue damage during straight and level flight was determined.

### **1.3.5 HELicopter Integrated Usage Monitoring HELIUM (H. Tijink, NLR)**

HELIUM is a secure data storage environment at the NLR and contains all relevant helicopter flight and loads/usage data generated by the RNLAf Chinook, Apache and Cougar helicopters and the RNLN NH90 helicopter. All types of data can be handled (FDR, HUMS, flight admin. data etc.). HELIUM is an XML database, with XPath and XQuery access to the stored data. Using XML documents as input for the data storage provides many advantages, such as easy conversion to and from XML documents, well defined syntax using XML Schemas, excellent support in e.g. Java, and a human-readable format.

HELIUM incorporates authentication, authorization and logging capabilities that allow extensive tracking and tracing of all actions performed in the database. A state-of-the-art work flow engine has been incorporated to facilitate recurring and tedious jobs such as standard reporting.

### **1.3.6 Reporting, Analysis and Visualisation Of Aircraft Lifecycle Information RAVIOLI (H. Tijink, NLR)**

A facility for reporting, analysis, and visualization of aircraft lifecycle information (RAVIOLI) is being developed to support military operators in loads, usage and maintenance monitoring. RAVIOLI is a fully integrated web-based toolbox with advanced tools for usage and health monitoring, prognostics, fleet life management and 3D simulation of actual flights.

RAVIOLI will work with helicopter data from HELIUM (see subsection 1.3.5) as well as allowing transparent access to other, already existing, flight data databases for the RNLAf C-130H and F-16 fleets. These databases have been in operation since the early 1990s and contain several terabytes of administrative and measured time series data.

As with HELIUM, RAVIOLI has advanced authentication, authorization and logging capabilities. These ensure that different types of users (e.g. maintenance engineers, weapon system managers, pilots) have the correct separation of access to different tools and data sets.

### **1.3.7 Stand Alone Structural data Acquisition system SALSA (A.B. Kloosterman, NLR)**

Currently available systems for load and usage monitoring are relatively large and require a costly and time consuming modification procedure before implementation. An alternative solution must be found when there is a need to quickly investigate local loading conditions in a structure. The NLR has therefore developed a miniaturised, stand-alone data acquisition system (SALSA) that can be rapidly deployed in practically every location in an aircraft. SALSA is designed and qualified for use in the RNLAf fleet with regard to temperature, altitude, humidity, accelerations, vibrations, shocks, EMI and EMC. The sampling rate is 1000 Hz and the system is able to store the strain data for 50 flight hours during a period of two weeks without human intervention. This is achieved by automatic measuring whenever a trigger signal due to aircraft usage is received from accelerometers inside the SALSA unit. The performance of the SALSA system has been demonstrated under operational loading conditions by temporary installation in an F-16. The system will become fully operational in 2009, see figure 8 and also subsection 1.3.1.

### **1.3.8 Structural fatigue load and usage monitoring of F-16 aircraft (F.C. te Winkel, NLR)**

Structural load monitoring of the RNLAf F-16 fleet is executed by NLR as a routine programme since 1990. During the nineties a completely new fatigue monitoring system specified by NLR was developed by RADA by extending their ACE pilot debriefing system with the loads and usage monitoring functionality: FACE (Fatigue Analyser & Air Combat Evaluation system). The main features of FACE are:

- The increase to five strain gauge locations: two indicative for wing root and “outer” wing bending, two at the rear fuselage dealing with horizontal and vertical tail loads, and one in the fuselage centre-section indicative for fuselage bending
- A flexible selection of flight, engine, and avionics parameters available via the MUX-BUS
- Fleet wide implementation (since 2003) allowing more extensive load monitoring of each individual aircraft.

The Crack Severity Index (CSI) is used as damage indicator. The CSI was developed by the NLR and is a relative measure of damage. For the F-16 a CSI value of 1.0 means fatigue damage according to the reference usage and loading environment used by LM Aero to generate the current inspection schedule (Fleet Structural Maintenance Plan, FSMP). The CSI method takes into account interaction effects between large and small load cycles (or between severe and mild flights). The CSI can be used as an indicative measure for ASIP (Aircraft Structural Integrity Programme) control points, since it is a relative figure between the actually measured and reference usage and loading environment.

Switching from a sampling load monitoring programme to fleet-wide individual load monitoring, combined with the flexible way of measuring a wide range of additional flight parameters, required a different approach to handling data and/or information. The NLR developed and implemented a customized information system for storing, managing, and analyzing the collected measured flight data from the on-board FACE system together with the administrative operational flight data from the RNLAf computerized maintenance/debriefing system IMDS. This centralized information system enables efficient data handling for *ad hoc* analyses as well as generating routine status reports for fleet management purposes.

A similar loads and usage monitoring programme has been implemented for the Belgian Air Force (BAF), whereby the information system was modified to serve both the BAF and RNLAf. For both air forces intensive Loads and Environment Spectrum Survey (L/ESS) measuring campaigns were carried out to collect data with the FACE system and enable LM Aero to provide an update of the FSMP. Modifications are being made to the information system to set up a loads and usage programme for the FACH (former F-16s RNLAf).

The currently proven benefits from the FACE system and dedicated F-16 information system are:

- Valuable instrumentation package for Force Management purposes (both ASIP and ENSIP)
- Valuable source for mishap investigation
- Very flexible instrumentation package (each aircraft in theory a “unique” test A/C)
- More often used for *ad hoc* recording purposes:
  - o detailed engine FAULT-code recordings
  - o flight departure margin study
  - o MFOQA (Military Flight Operations Quality Assurance) trial 2007 with 18 dedicated A/C instrumented with dedicated measurement profile (FDM SCF)
- Information system is frequently used as a study for development of next generation decision support tools.

The capabilities in progress/under development are:

- Cumulative CSI for 5 strain gauge locations
- Linkage of CSIs to (clusters of) control points
- Flown store configuration in combination with g and speed level-crossings
- Gross weight tracking (4% IGW)
- LCO (Limit Cycle Oscillation) tracking capability
- Efforts to further increase capture rate
- Fuel consumption
- Dedicated Landing Gear Damage Indicator.

### 1.3.9 Structural health monitoring AHMOS-II (J.H. Heida, NLR)

(1) General scope. The NLR participated in the ERG 103.015 programme “Prototype Demonstration of Modular Structural Health Monitoring System for Military Platforms (AHMOS-II)” conducted in 2004-2008. The AHMOS-II consortium consisted of eighteen Industrial Entities from seven European countries and successfully achieved the following objectives:

- Development of practical sensors and extended capability of sensors in a modular system network environment for future Structural Health Monitoring Systems (SHMS)
- Demonstration of an operational prototype SHMS based on mature-enough sensing techniques: flight testing supported by independent full-scale on-ground damage detection tests
- Assessment of reliability in operational environment, cost benefit, and possibility of replacing conventional inspection procedures.

Five sensor technologies were selected and integrated into a prototype modular networking SHMS with user interface for data presentation. The sensor technologies underwent an airworthiness programme and were demonstrated to a technological maturity level of TRL7 (i.e. “prototype in operational environment”), thereby proving that the core competencies are capable of bringing the technologies to their final form.

(2) NLR contributions. The NLR’s main activities in the AHMOS project included the following:

- *Central computer for data acquisition*

A central computer for data acquisition (remote data concentrator) was developed. The hardware is a COTS-based PC104 solution, and the software runs under the VxWorks operating system. The central computer features a web-based user interface enabling real-time monitoring of all the sensor subsystems and the network, using any web browser on a connected laptop. The NLR central computer was installed in the pod of a Hawk aircraft for flight testing in the UK, together with other AHMOS-II system components, see figure 9.

The flight tests were successfully conducted in July 2007. Integration of the central computer with the other system components on the network and data exchange levels was successful. During the flight tests the central computer performed as designed. The web-interface of the central computer was found to be an integral part of the flight tests. It was used prior to and after each flight to ascertain the status of the equipment boxes, i.e. were the boxes in "operational" mode prior to each flight and were they still "operational" on landing.

- *Development of eddy current array sensors*

An investigation was made into the feasibility and potential applicability of eddy current (EC) sensors for local monitoring of critical areas in metal aircraft structures. Two prototype EC sensors were developed: a thin and flexible high-frequency absolute sensor, figure 10, and a low-frequency reflection ring sensor, figure 11. The sensors were evaluated using a range of test specimens containing artificial defects and fatigue cracks, also including specimens under actual fatigue loading.

The investigation showed that the high-frequency sensor is suited to detecting surface cracks located just beneath the sensor. The sensor is flexible and can be bent down to small radii, producing reliable EC signals for radii down to 7 mm. The low-frequency ring sensor is suited to detecting sub-surface cracks in riveted joint structures. The detectable crack length for this sensor depends on the inspection configuration, the depth of the defects and the test frequency. As a rough indication, defects  $\geq 8$  mm long and at a depth up to 3 mm are detectable in lap joints of the fibre/metal laminate GLARE (GLASS REinforced aluminium laminate) See also subsection 1.4.1 for reference to similar topics.

- *Data analysis methods*

A review was made of different data analysis methods that can be used for SHM techniques. Basic steps in signal processing include data pre-processing, data analysis by transforming to different domains, and data post-processing. The most important sensor techniques were discussed and appropriate signal processing techniques were reviewed. In addition, the applicability of specific data analysis methods for five relevant SHM techniques was discussed.

Besides these main activities the NLR was responsible, together with Fokker Services, for evaluating all of the AHMOS-II key systems. All ground test, flight test and investigation results were evaluated in order to determine the status with respect to fulfilling the functional, qualification and maintenance requirements. Aspects of the evaluation included the main detection/research objective of the individual systems (impact damage, surface crack, sub-surface crack around fasteners, skin-stiffener debonding, residual stress, chemical sensing, etc.); the TRL rating and its substantiation (e.g. in cases where a relatively low TRL was caused by failure of other sub-systems); and the main advantages and limitations of the systems. The next steps for improvements and exploitation of SHM were indicated.

### 1.3.10 Comparative vacuum monitoring (J.H. Heida, NLR)

An evaluation of the comparative vacuum monitoring (CVM) technique for fatigue crack detection has been done using a CVM laboratory system, figure 12. The CVM technique is based on the principle that a small volume maintained at a low vacuum ( $\sim 0.7$  atm.) is extremely sensitive to any ingress of air, e.g. via a crack, see figure 13. Basic features of the inspection technique were described and a literature study on CVM applications was made, followed by measurements for friction stir welded (FSW) stringer panels under fatigue and static loading. It was found that the sensors were easily applied and attached well to the specimen surfaces.

- (1) Fatigue. Fatigue testing evaluation showed that the CVM laboratory system is easy to use and has a high sensitivity for crack detection, which occurs when the crack tip reaches the first vacuum channel of the CVM sensor. No false calls were obtained during the complete testing period.
- (2) Static loading. Under static loading conditions the CVM measurements were less successful, most probably because of residual compressive stresses in the FSW panels (up to 40 MPa). It seems that the CVM system can only properly detect cracks when they are open. For closed cracks the detectability is minimal.

For the time being, CVM application on RNLAf aircraft structures is intended to be off-line on the ground (periodic inspection at predetermined intervals). In this situation the CVM technique should only be used for structural parts known to be under tension loading.

A new and portable version of CVM equipment (PM200) has recently been developed by SMS Ltd. for in-service use on aircraft. The PM200 is claimed to be more sensitive for crack detection and less sensitive for environmental influences. It is probably also less sensitive to crack closure. A further evaluation of the CVM technique, using both the laboratory system and the PM200 system, will be carried out in the next ICAF reporting period.

## 1.4 FIBRE/METAL LAMINATES (FMLs) FULL AND SUB-SCALE TESTS

### 1.4.1 GLARE Teardowns from the MegaLiner Barrel Fatigue Test (P.H. de Haan, NLR)

The pressure cabin MegaLiner Barrel (MLB) fatigue test was part of the Airbus A380 development programme. The NLR carried out teardowns of GLARE structures from three key locations of the MLB: a window area, a beam above the passenger door, and some stringer couplings. The teardowns began with Non-Destructive Inspection (NDI), and were followed by fractographic investigation of NDI-indicated cracks in the window and door beam locations. The main objectives were to verify the NDI techniques and capabilities, determine the fatigue initiation and crack growth behaviour, and provide data to check fatigue crack growth models for GLARE.

As discussed in a paper presented at the 25<sup>TH</sup> ICAF Symposium [3], the overall results demonstrated very good NDI teardown capabilities and high fatigue damage tolerance by the GLARE structures. The window area fatigue cracks were too small to check model predictions, but a significantly longer door beam crack had a virtually constant growth rate, which agrees with model predictions. Figure 14 shows the fractographically-obtained crack growth rate data.

#### 1.4.2 Fatigue and damage tolerance tests on a curved GLARE fuselage panel (W. van der Hoeven, NLR)

This project had the main objective of demonstrating that thin GLARE skins can be used for the pressure cabins of narrow-body jet aircraft such as the Airbus A320 successor. A 3030 mm long and 1185 mm wide curved GLARE panel was designed by Stork Fokker and the NLR. Figure 15 gives a schematic of the panel. The geometry is based on the A320 fuselage structure, and the panel consisted of two sections connected by a circumferential butt joint (which was not a test item).

Most of the panel components were assembled by Stork Fokker. The skin was two kinds of thin GLARE 3: one section had a 0.85 mm thick standard GLARE 3-2/1-0.3 skin, made with 0.3 mm thick Al 2024-T3 sheets; the other had a GLARE 3-2/1-0.35 skin made with 0.35 mm thick aluminium lithium (Al-Li) alloy sheets. Along the panel centre line there were two kinds of longitudinal joint: the standard GLARE skin had a friction stir welded (FSW) joint; the Al-Li GLARE skin was joined using a standard bonded overlap splice, see figure 16. The stringers were GLARE 2, and the frames were a standard monolithic aluminium alloy. The stringers were not interrupted at the butt joint.

Static and fatigue tests were performed on the panel using the NLR fuselage test rig, figure 17. This rig enables testing under simulated cabin pressurization, combined with axial tensile loads to simulate fuselage bending owing to gusts and manoeuvres. The static tests were done first, in order to assess the strain distribution in the panel.

The fatigue testing was performed in two parts:

- (1) Fatigue crack initiation. The first part consisted of 90,000 simulated flights using a simple spectrum with once-per-flight loads only. The loads were set at conservatively high levels. The panel was thoroughly inspected during and after this part of the test. The only detectable damages were NDI indications of three tiny cracks in the outer aluminium layer of the FSW. The presence of these cracks could not be confirmed visually.
- (2) Damage Tolerance (DT). Before DT testing the panel was impacted at several locations. The impact energies were selected such that damages, in the form of small cracks, were created in one of the aluminium layers of each GLARE skin section. Fatigue testing continued using a conservatively scaled A320 fuselage flight simulation spectrum supplied by Airbus. This spectrum included axial loads.

The impact damage was monitored during the first 45,000 simulated flights, but no crack growth occurred. However, several additional crack indications in the FSW were found. Subsequently, several 30 mm long sawcuts were introduced into the skin at the impact locations. In addition, one of the stringers (and skin) was cut at one location in each skin section.

The DT test was resumed and the sawcuts were monitored for fatigue crack growth. After an additional 15,000 simulated flights an artificial hole (60 × 60 mm) was made at a critical location and then “repaired” with a hot bonded patch. The test continued up to a total of 105,000 simulated flights, when it had to be stopped because one of the sawcut-initiated fatigue cracks approached the panel edge (total crack length about 350 mm). Besides the growth of sawcut-initiated fatigue cracks the only other additional damages were several more crack indications in the FSW.

Finally, a limited teardown inspection was done. Several rivets were removed and inspected with an eddy current rotor probe. During this inspection only one tiny fatigue crack was found in one of the holes. Sections of the FSW were cut out for microscopic investigation.

In the light of all the results, and also the conservatively high fatigue load levels, it was evident that the thin GLARE skin structure showed a high degree of damage tolerance and would most probably meet all DT requirements for a narrow-body pressure cabin. The DT test also demonstrated the reparability of a thin GLARE structure, since no debonding or cracking occurred along the edges of the “repair” patch. The only negative aspect was (limited) cracking in the friction stirred welds. Before FSW splices can be used the welding quality should be improved.

#### **1.4.3 Fatigue and static tests on a GLARE stringer coupling panel (W. van der Hoeven, NLR)**

This project had the main objective of evaluating the fatigue and residual static strength behaviour of stringer couplings on a stiffened GLARE panel. The panel was designed and manufactured by Stork Fokker and the TUDelft, and simulated a circumferential joint in the upper fuselage section of an A320 type of aircraft.

Figure 18 gives a schematic of the panel, which was flat rather than curved. Owing to the panel’s limited width, simulation of the curvature in an actual structure was not considered necessary. The skin was GLARE 3-3/2-0.3. The skin was stiffened by GLARE stringers on one side of the circumferential joint, and by extruded aluminium lithium (Al-Li) stringers on the other side. At the joint the skin sections were connected using a GLARE 2 butt strap and the three pairs of stringers were connected by different GLARE stringer couplings. A frame was attached to the butt joint to improve the simulation. Note also that the GLARE skin was attached to aluminium clamping plates via the stringer runouts.

The panel was equipped with several strain gauges to measure the strain distribution. Prior to fatigue testing, two static tests were performed to measure the strain distributions. One test was done with frame support and one without it. The strain measurements indicated that the frame support conditions had a significant effect on the strains in the stringer couplings, and subsequent testing was done with frame support, see figure 19.

Fatigue testing was done under constant amplitude loading representing once-per-flight longitudinal loads, and to a total of 195,000 cycles, representing three A3X0 design lives. During the test the panel was regularly inspected for fatigue cracks at the fastener holes. However no cracks were found. After the test several fasteners were removed to inspect the holes more thoroughly, but again no cracks were found.

After fatigue testing, an ultimate load test was performed. During this test the panel failed in the unreinforced section of the GLARE skin. This unexpected failure mode was due to failure of the rivets in the stringer runouts joining the GLARE skin to the clamping plates, figure 20. Owing to the rivet failures the overall failure load was well below the ultimate design load. However, since the panel was free of fatigue cracks and the strains in the stringer couplings and butt strap were still low when the panel failed, it was concluded that the stringer couplings would probably have sustained ultimate load without the unexpected failure.

#### **1.4.4 Static and fatigue tests on GLARE panels with bonded and riveted repairs (W. van der Hoeven, NLR)**

This project had the main objective of demonstrating that thin GLARE fuselage skins can be repaired. Two flat panels simulating sections of a fuselage skin were “repaired”. One panel had a bonded repair and the other had a riveted repair. For both panels the skin was a GLARE 3-2/1-0.3 laminate with a thickness of only 0.85 mm.

The panels were manufactured by Stork Fokker and FMLC and tested by the NLR. Each panel underwent two static tests. The first tests were to show that the panels could sustain the ultimate design load, and the second tests were to determine the failure loads. The bonded repair panel was also fatigue tested between its two static tests, and both panels were artificially damaged (impacted and/or scratched) just before the second static tests.

During the first tests both panels sustained the ultimate design load (200 kN) with some plastic deformation of the Glare 3-2/1-0.3 skin, but otherwise no visible damage development. During the second tests both panels failed well above the ultimate load: the bonded panel failed at 375 kN from an artificial scratch, 0.1 mm deep, but without cracking or delamination associated with the patch; the riveted repair panel failed at 280 kN along a pre-existing crack due to impact.

## 1.5 FIBRE/METAL LAMINATES (FMLs) SPECIMEN TESTS

### 1.5.1 Fatigue crack growth in FMLs under variable amplitude loading (S.U. Khan, R.C. Alderliesten, TUD)

The major objective of this research is to develop the understanding of variable amplitude (VA) fatigue crack growth in FMLs. Subsequently, an analytical fatigue crack growth model will be developed to enable crack growth predictions. To quantify the crack growth mechanism the project is divided into two main subcategories:

- (1) Delamination under variable amplitude loading. Delamination fatigue tests were done with a doubly-cracked lap shear specimen subjected to simple block loading, programmed block loading and flight loading sequences. The purpose was to analyse the effect of VA loading on delamination growth rates in FMLs. The left-hand diagram in figure 21 compares an example of the effects of multiple block loads with HI-LO and LO-HI sequences. This diagram illustrates that delamination growth rates are the same at each stress level, irrespective of the load sequence. In other words, there are no history and interaction effects during delamination in FMLs.
- (2) Crack growth prediction and analytical model development. FMLs have metal layer crack growth characteristics similar to those in monolithic metals, although crack growth is much more restricted owing to fibre bridging. The crack growth prediction methods currently being developed for FMLs account for the similar characteristics by implementing interaction models developed for metals. At the present time two models have been implemented, one based on linear damage accumulation and the other based on a yield zone model. The right-hand diagram in figure 21 shows that the model predictions correlate fairly well with experimental results. However, several detailed phenomena are still being investigated.

### 1.5.2 Delamination growth at interfaces in hybrid materials and structures under various opening modes (G. Delgrange, R.C. Alderliesten, TUD)

This project focuses on mode I and mode II delamination in FMLs under fatigue loading. The objective is to obtain a Paris-type relation for the delamination of hybrid materials as function of the strain energy release rate.

- (1) Specimens. Figure 22 shows the specimen configurations. For mode I loading the double cantilever beam (DCB) test was chosen. For mode II loading the end-notched flexure (ENF) test was selected. The specimens were cut from a GLARE 2A-2/2-0.4 panel. Two external doublers made of Al 7075-T6 (thickness 4.1 mm) were bonded on both sides of the specimens to prevent plasticity invalidating the expressions for the strain energy release rate.
- (2) For mode I the delamination occurred randomly at one or both interfaces between the fibres and the aluminium layers. Figure 23 is a plot of delamination growth as a function of the energy release rate of the interface for several tests done with different displacement amplitudes,  $d$ . There is a consistent Paris-type relation, i.e. a linear trend on a log-log plot of  $da/dN$  (delamination growth rate) and the maximum strain energy release rate,  $G_{max}$ .
- (3) For mode II the trend is not as clear as for mode I. Each test resulted in only a small amount of delamination, and variations between specimens tested with different displacement amplitudes led to discrete sets of data rather than a continuous plot, see figure 24. On the other hand, there seems to be an indication of a mode II threshold value of strain energy release rate, indicated by 'G no delamination'. The value of ' $G_{crit}$ ' is derived from the static test.

Based upon these observations it is concluded that the delamination behaviour during fatigue has been characterized quite well for mode I loading, while a trend has been obtained for mode II. Some mixed mode loading experiments should now be done to understand the contribution of each mode. Later on, these contributions could be included in design criteria and a numerical model.

### 1.5.3 Effective strain energy release rate for fatigue delamination (R. Khan, C.D. Rans, TUD)

For composite laminates the delamination growth during fatigue is often characterized by the maximum strain energy release rate,  $G_{max}$ , or by the difference in strain energy release rate for the applied load cycle,  $\Delta G$ . The use of strain energy release rate instead of the stress intensity factor,  $K$ , relates to the difficulty in determining  $K$  for complex

laminates. However, translating from a  $\Delta K$ -description of fatigue crack growth to a  $G_{\max}$ - or  $\Delta G$ -description of delamination growth is not logical.

Use of  $\Delta K$  as a parameter for crack growth is based on a Linear Elastic Fracture Mechanics (LEFM) assumption and the adoption of a similitude concept, whereby similar crack tip stress amplitudes (related to the remotely applied stress amplitudes) result in similar crack growth rates. Translating this similitude principle to delamination growth results in an alternative formulation for an effective strain energy release rate (for single mode loading), based on the superposition rules of  $G$ :  $G_{\text{eff}} = (\sqrt{G_{\max}} - \sqrt{G_{\min}})^2$ . Using this formulation to describe Mode II delamination growth in FMLs gives more generic descriptions of fatigue delamination growth that are independent of residual stress and hence stress ratio ( $R$ ) effects, see figure 25. Furthermore, using this formulation to describe delamination behaviour in other loading modes will allow any observed variations to be investigated based upon the same similitude principle used for crack growth, i.e. the similitude of the remotely applied stress amplitude.

#### 1.5.4 Fatigue crack growth in CentrAl (G. Wilson, R.C. Alderliesten, TUD)

The TUD's already strong experimental and analytical understanding of crack growth in FMLs such as GLARE and ARALL (Aramide Reinforced ALuminium Laminates) is being extended to laminates. CentrAl is a new FML that provides the right mix of properties and ease of manufacturing for thicker aircraft structures such as a lower wing skin. CentrAl is made up of thicker aluminium sheet, internal GLARE reinforcement and fibre glass prepreg, see figure 26. CentrAl laminates with aluminium layers up to 2 mm thick have been tested, and many advanced aluminium alloys can be used that would be unsuitable for thinner FMLs.

Two approaches are simultaneously being employed to describe fatigue crack growth in CentrAl, one empirical and one analytical:

- (1) The empirical approach relies on the phenomenon that cracks in the outer sheets of CentrAl grow at a nearly constant rate that depends on the loading conditions but not the length of the crack. Figure 27 is an example of how constant the fatigue crack growth rate can be.
- (2) The analytical approach involves extending the analytical model developed for fatigue crack growth in GLARE to a generalised laminate, with arbitrary composition, independent cracks in each metal layer, and independent delaminations between layers. The extended model determines the crack bridging stresses along each interface and simulates the growth of each crack according to these stresses.

#### 1.5.5 Preliminary study of the effect of prestraining on the fatigue crack growth properties of Zylon FMLs (W. van der Hoeven, NLR)

Owing to their high stiffness, Zylon fibres are being considered as possible replacements for S2-glass fibres in FMLs, notably for FML stringers in the upper crowns of GLARE fuselage structures. A disadvantage of Zylon fibres is the negative thermal expansion coefficient, which results in relatively high thermal stresses in the laminates after curing the prepreg adhesive at elevated temperatures. The thermal stresses in the aluminium layers are tensile stresses and would probably be detrimental to the fatigue crack growth properties of the laminates. This is a general problem for FMLs, but the use of Zylon fibres poses another problem, namely the possibility of buckling failure of the fibres bridging a fatigue crack in the aluminium sheets. There are two reasons why fibre buckling could occur:

- (1) The fibres are organic, consisting of bundles of fibrils that could buckle under compressive (fatigue) loading.
- (2) The presence of thermally-induced compressive stresses in the fibres after curing.

These considerations led to the present study, to see whether prestraining the laminates after curing would ameliorate or avoid fibre buckling during fatigue crack growth. Tests on non-prestrained and prestrained Zylon FML2 specimens containing crack growth starter notches were performed. One non-prestrained and one prestrained specimen were fatigued at a maximum stress,  $S_{\max}$ , of 180 MPa and with stress ratio  $R = 0.1$ . In addition, one non-prestrained and one prestrained specimen were tested with the same stress range ( $\Delta S = 100$  MPa) but with a negative stress ratio,  $R = -0.3$ . During the tests the crack growth was monitored. After testing, the delamination zones in the vicinity

of the fatigue cracks were made visible by removing the outer aluminium sheets of the laminates.

The tests with  $R = 0.1$  showed that fibre failure did not occur. Even so, prestraining resulted in a large reduction in fatigue crack growth rates. The crack growth rates in the non-prestrained specimen were comparable to those in GLARE 2 specimens.

The tests with  $R = -0.3$  were more discriminating. Figure 28 gives an example of the crack growth results. Fibre breakage occurred during crack growth in the non-prestrained specimen, resulting in a steady increase in crack growth rates. However, prestraining prevented fibre breakage. This had a very large and beneficial effect on the fatigue crack growth behaviour, with a strong indication of eventual crack arrest. The beneficial effect of prestraining was attributed to the introduction of (additional) residual tensile stresses in the fibres.

The overall results showed that the fatigue crack growth properties of Zylon FMLs are probably not much better than those of standard GLARE laminates. However, Zylon FMLs have to be prestrained to prevent fibre failure during compressive fatigue load cycles. Prestraining is also required for obtaining high stiffness of the laminates.

## 1.6 FATIGUE AND DAMAGE TOLERANCE STUDIES

### 1.6.1 Automated Transfer Vehicle (ATV) panel hinge (P.H. de Haan, NLR, G.A.M. Vermij, Dutch Space)

An Automated Transfer Vehicle (ATV) panel hinge specimen was subjected to fatigue damage tolerance tests using load sequences derived from the Jules Verne (JV) and ATV spectra. Figure 29 shows the specimen, which was an aluminium alloy double lug design, with one male and one female lug. Corner-crack starter notches were electric discharge machined into the lugs at the locations Da-Db and Fc-Fd to side surface depths of 1.64 mm and 1.36 mm, respectively. The specimen was statically and fatigue tested in an *ad hoc* rig as shown in figure 30.

The test programme consisted of two static tests, four fatigue life tests with the JV spectrum and four fatigue life tests with the ATV spectrum. The first static test was done before fatigue testing. The second static test was done during the second JV fatigue life test. The panel hinge specimen was required to complete all the tests without (a) complete failure, i.e. both lugs failed, and (b) crack initiation elsewhere in the component. During the test programme the notches at Da-Db extended by fatigue until failure of (one-half of) the female lug. However, no crack growth occurred from the notches at Fc-Fd, and there were no other cracks. Hence the damage tolerance capability of the panel hinge was considered to be validated.

### 1.6.2 Fatigue research on Friction Stir Welding (FSW) (H.J.K. Lemmen, R.C. Alderliesten, TUD)

Friction Stir Welding (FSW) is a joining technology which can improve the efficiency of aircraft structures. However, the technology is not mature, and the fatigue behaviour of friction stir welds must be fully understood before they can be used in damage tolerant aircraft structures. At the 24<sup>TH</sup> ICAF Symposium a paper was presented about the fatigue initiation properties of FSW joints in Al 2024-T3. There was also some limited information about the fatigue crack growth behaviour, notably an out-of-plane deviation of the crack growth direction, see figure 30.

Because the fatigue crack growth rates and crack growth directions greatly depend on the mechanical properties of friction stir welds, two investigations were conducted:

- (1) Local yield strength and residual stresses. A new measurement method, Digital Image Correlation (DIC), was used to obtain the local yield strength and residual stresses associated with a friction stir weld. DIC uses the images taken from a specimen to measure its deformation. This was the only way of obtaining a detailed strain field, and hence the local mechanical behaviour, including the local yield strength. The results are shown in figure 32 for FSW in three aluminium alloys, Al 2024-T3, Al 7075-T6 and Al 6013-T4, which are standard alloys used in the aircraft industry.
- (2) Fatigue crack growth. Centre Cracked Tension (CCT) specimens of the same three alloys, with friction stir welds, were prepared for fatigue crack growth testing. The tests involved FSW in different configurations, namely

specimens with welds at angles of 0°, 45° and 90° with respect to the applied load direction. Images for DIC analysis were taken from the specimens at fixed fatigue life intervals. These images were analysed to obtain the strain fields around the crack tips.

The results showed exceptional fatigue crack growth behaviour, e.g. figure 33. It is believed that the local yield strength and residual stresses have a large influence on the plastic zone in front of a crack tip. Whereas the plastic zone originally has a butterfly-shaped geometry, this is changed dramatically when the fatigue crack grows into a friction stir weld. Firstly, the yield strength will change the geometry of the plastic zone, and hence the effects of fatigue crack closure. Secondly, the residual stresses will change the orientation of the principle stress and hence the direction of fatigue crack growth. The residual stresses will also affect the strain field in front of the crack tip.

The complete findings from this test programme are discussed in a paper presented at the 25<sup>TH</sup> ICAF Symposium.

### 1.6.3 Friction stir welded stiffened panels (F.P. Grooteman and L. 't Hoen-Velterop, NLR)

The NLR participated in the European project DaToN, whose main objective was to provide basic knowledge and assessment tools for damage tolerance evaluation of integrally stiffened structures. Integral stiffening is obtained by three modern production methods: high speed machining, laser beam welding and friction stir welding (FSW).

These types of structures have very different crack growth properties compared to the more traditional riveted and bonded structures. The main problem for integrally stiffened structures is the crack arresting capability of the stiffeners. In the case of laser beam and friction stir welding there are also effects due to the residual stress fields.

Within the DaToN project the NLR examined an engineering prediction method to compute the residual stress field in FSW joints and stiffened panels. A parametric MSC.Patran PCL script was developed to quickly calculate the stress intensity factor as a function of crack length for an integrally stiffened panel having two T-stiffeners. With given values of the geometry parameters the script automatically generates a set of MSC.Nastran input decks for the various crack lengths, including the crack tip elements. These files are run and automatically processed to obtain the stress intensity factor. Figure 34 shows an example calculation.

Also, three different stress distribution functions, modelling the residual stresses in the FSW weld line direction were implemented in the crack growth package NASGRO and examined for accuracy. One of these showed a good correlation with experimental data.

Finally, several friction stir welded panel configurations were analysed with the parametric finite element model to determine the normalised stress intensity factor. Crack growth was analysed with NASGRO using this stress intensity factor together with the implemented residual stress distribution. The obtained crack growth lives were compared with experimental data.

### 1.6.4 Modelling Frictional Load Transfer in Mechanically Fastened Joints (L. Paletti, C.D. Rans, TUD)

Fatigue models for mechanically fastened joints focus primarily on net-section fatigue failures associated with high pin-bearing loads, bypass load, and the exacerbating effect of the stress concentration of the fastener hole. In some joint applications, particularly where high fastener clamping is present, fretting-induced fatigue failure occurs, and this is associated with frictional load transfer in the joint. Although separate fatigue models exist for both fretting and net-section fatigue, existing load transfer models for mechanically fastened joints typically neglect friction, making it difficult to determine when fretting fatigue failures are expected to be dominant.

A new load transfer model that considers friction is being developed to provide a means of assessing the dominant fatigue mechanism present in a mechanically fastened joint. By modelling the frictional load transfer using a Hertzian contact assumption a splitting factor between frictional and bearing load transfer can be determined as a function of applied load and fastener clamping. This splitting factor can then be related to the dominance of either fatigue mechanism. Currently the developed model only applies only to mechanically fastened joints without secondary bending. Figure 35 shows an example of the model predictions.

### 1.6.5 Fatigue of structures and secondary bending in structural elements (J. Schijve, G. Campoli, A Monaco, TUD)

Secondary bending occurs in structural elements loaded in tension when eccentricities are present. Two important examples are lap joints and plates with locally increased thickness [4]. Owing to the eccentricities, out-of-plane displacements occur and result in local bending. This phenomenon is unfavourable for the fatigue properties of a structure. Secondary bending should be considered for designing against fatigue, but it has received limited attention so far:

- (1) Lap joints. Secondary bending has been analyzed with FE calculations and also with a neutral line model. A bending factor  $k_b$  is defined as the ratio of the bending stress and the nominally applied tensile stress. The secondary bending depends on the dimensions of the lap joint: values of  $k_b$  larger than 1 can occur, and lower  $k_b$  values can be obtained by increasing the overlap of the joint.
- (2) Local thickness increase. FE-calculations were made for an open hole with a reinforced edge around the hole, see figure 36, which shows that the stress concentration is significantly increased by secondary bending due to non-symmetric reinforcement. Figure 37 shows the out-of-plane displacements.

### 1.6.6 Fatigue crack marker loads in aerospace alloys (S.A. Barter, DSTO Melbourne, R.J.H. Wanhill, NLR)

The selection of fracture surface marking methods based on exploiting or altering the required fatigue loads is of much interest for many fatigue test programmes. This is particularly true when crack growth measurements during testing are not possible or insufficiently accurate. In such cases, post-test Quantitative Fractography (QF) of the fatigue crack growth may then be needed, and this can be made possible and/or greatly facilitated by fracture surface markers. A joint DSTO – NLR report has been prepared to review the various fracture surface marking methods and obtain guidelines and procedures to optimise their use for QF of fatigue crack growth [5]. Numerous examples are provided to substantiate the guidelines, e.g. figure 38.

### 1.6.7 Substantiation of lug details for single load path primary structures ACCOLADE (P. Nijhuis, NLR)

Use of composite single-load-path primary structures on aircraft requires demonstration of the proof of concept. This can be very expensive, for example the costs to demonstrate that a complete composite brace meets the fatigue and damage tolerance requirements of FAR 25.571.

Costs in demonstrating the proof of concept for generic composite braces can be reduced by testing lug details separately. The project ACCOLADE (Affordable Composite Component for LAnDing gEar) involved moisture absorption, strain verification and fatigue tests on lug details, see figure 39. The lugs were manufactured with artificial delaminations and subjected to high-speed impact damage before fatigue testing, which was done at different temperatures. The lug details met all the fatigue and damage tolerance requirements and therefore demonstrated the proof of concept of a generic composite brace.

### 1.6.8 High-cycle fatigue of laser beam deposited Ti-6Al-4V and Inconel 718 (E. Amsterdam, NLR)

Laser powder deposition is an innovative and rapid prototyping technique for metals. The technique uses a laser to create a melt pool on a substrate and metal is deposited onto the substrate by injecting metal powder through a nozzle into the melt pool. The melt pool is shielded from oxygen by inert gas. Rapid cooling solidifies the deposit while the substrate is sweep-scanned back and forth according to a 3D Computer Aided Design (CAD) pattern. A *complex* 3D component can be created by adding multiple layers.

For application to critical aircraft structure or gas turbine parts the status of the technology has to be assessed by determining the microstructure and mechanical properties of relevant aerospace alloys. Two identical thick-walled components have been fabricated from the “workhorse” titanium and nickel-base alloys Ti-6Al-4V and Inconel 718. The components were given standard heat treatments prior to cut-up for machining smooth (unnotched) fatigue test specimens.

High-cycle S – N fatigue tests,  $R = 0.1$ , were done to  $5 \times 10^7$  cycles. Both alloys had fatigue limits similar to those of equivalent wrought alloys. This was despite the fact that the fracture surfaces showed small pores, especially in Inconel 718.

## 1.7 FULL-SCALE AND DETAIL FATIGUE TESTING

### 1.7.1 Low-cycle fatigue spectrum and test for the NH90 helicopter tail module (E. Mantel, T. Janssen, Stork Fokker AESP B.V.)

The NH90 helicopter tail is a hybrid structure consisting of composite panels and aluminium parts. The fatigue loads are both low-cycle and high-cycle. The low-cycle spectrum originates from the mission types: the main contributors are flight loads from the horizontal stabilizer, vertical fin and tail rotor, and the ground-air-ground cycles. The high-cycle fatigue loads come from the vibrations imposed by the dynamic system of the helicopter.

Safety aspects require compliance with FAR 29.571. The necessary fatigue substantiations are a mix of approaches based on flaw tolerant safe-life, multiple load path damage tolerance, and, if unavoidable, safe-life. These substantiations are supported by full-scale and detail testing.

Figure 40 is a view of the full-scale test set-up, which is in the new Test Hall at the NLR. Prior to testing there has been much research into the flight spectrum characteristics, as mentioned in the previous ICAF Review. For example, the aluminium hinge connecting the foldable composite tail module with the rear of the main structure is subjected to low-cycle fatigue coming from ground-air-ground cycles and in-flight loads. A realistic low-cycle fatigue spectrum was obtained by combining simulated landing responses with a flight-by-flight spectrum, for which the loads were retrieved from an extensive in-flight measurement programme. The flight-by-flight and landing spectra were derived by Stork Fokker. The flight spectrum is based on a number of different flight types arising from mission definitions. The landing spectrum is based on a landing speed distribution and is representative for a set of landing conditions such as weight, roll and pitch attitudes, etc. The load sequencing within each flight type as well as the occurrence-mix of the different flight types were also derived by Stork Fokker.

To obtain an efficient test spectrum for the full-scale test the spectrum has been reduced to a subset of critical loading conditions. Small cycles were omitted as well as infrequent peak loads. The spectrum reduction is driven by the aluminium structure, but checked to be severe enough for the composite structure as well (compression-compression cycles). Apart from these conditions, the flight and landing loads are randomly distributed with respect to the total number of occurrences and flight segment sequences.

The test consists of 2 main phases:

- (1) Fatigue testing to demonstrate compliance with the service life requirements and safe-life requirements. This test phase covers the following damage levels: as-manufactured metal parts and BVID in the composite parts.
- (2) Fatigue testing to confirm safe inspection intervals. This test phase covers higher levels of damage: artificial damage in metal parts and CVID in the composite parts.

Various residual strength tests will be included between the fatigue test phases and at the end of the total test.

### 1.7.2 High-cycle fatigue test on NH90 helicopter tail hinge lugs, including flaw tolerance (T. Janssen, Stork Fokker AESP B.V.)

In-flight helicopter manoeuvres are characterized by high frequency dynamic loads (with occurrences as high as  $10^9$  per helicopter life) superimposed on quasi-stationary fatigue cycles (low-cycle fatigue). When applicable, damage tolerance for the NH90 helicopter tail structure is substantiated by residual fatigue strength in a multiple load path analysis with 1 failed element and compliance with the required repeat inspection intervals.

For items unsuitable to the above approach, such as the tail hinge lugs, high frequency fatigue tests with artificially flawed specimens were performed to meet the damage tolerance requirements. The fatigue endurance properties of the hinge lugs are enhanced by installation of FTI Forcemate™ bushes in the lug holes, see figure 41. The Forcemate bushes result in cold expansion of the holes, and the high interference reduces fretting. Both of these aspects help to increase the average fatigue life.

Under contract to Stork Fokker, the NLR performed constant amplitude specimen tests to quantify the change in fatigue life resulting from the Forcemate process. Tests were done up to 60 million ( $6 \times 10^7$ ) cycles. The test results enabled producing safe S-N design curves, for both pristine and artificially flawed lug holes, to be used when analyzing the high-cycle fatigue life of lugs fitted with Forcemate bushes.

## 1.8 SPECIAL CATEGORY

### 1.8.1 Fatigue of Structures and Materials (J. Schijve, TUD)

A second edition of the textbook with the above title has been published by Springer in January 2009. The second edition is a revised follow-up of the first edition printed in 2001. The book is a textbook for universities, research institutes, and industries. The major part of the first edition has been maintained, but in the second edition there is a fully rewritten chapter about designing of structures against fatigue. A major supplement of the new edition is the CD now added to the book. It contains exercises and hints for answers which are useful for courses and self-tuition. Furthermore, it includes case histories of fatigue problems and information on specific topics covering designing against fatigue, prediction scenarios, fatigue experiments (how and why?), fractography, and research in the future. A survey paper by the author about research on fatigue problems in the 20th Century is also on the CD.

### 1.8.2 Creep-fatigue damage in single crystal Ni-base alloys (T.Tinga, Netherlands Defence Academy)

A damage model for single crystal Ni-base superalloys was proposed [6]. The model integrates time-dependent (creep) and cyclic (fatigue) damage into a generally applicable time – incremental damage rule. A criterion based on the Orowan stress was introduced to detect slip reversal on the microscopic level, and the cyclic damage accumulation was quantified using the dislocation loop immobilization mechanism. Further, the interaction between cyclic and time-dependent damage accumulation was incorporated into the model. Implementation in a multi-scale constitutive framework for Ni-base superalloys enables simulations for a wide range of loading conditions and shows adequate agreement with experimental results.

### 1.8.3 Some notable aircraft service failure investigated by the NLR (R.J.H. Wanhill, NLR)

A review was made of several notable aircraft and aeroengine service failures investigated by the NLR since the mid-1970s [7]. These failures were chosen partly to illustrate the specialist knowledge required for determining the physical causes of failure, but attention was also paid to the broader aspects of structural safety and preventing additional failures. The selected failures were: Sikorsky S-61N helicopter rotor blade (1974); General Electric CF6-50 G40 turbine blades (1977-9); Air Tractor AT-301 propeller blade (1987); Aérospatiale Alouette III helicopter tail lug (1990); General Dynamics F-16 / Pratt & Whitney F100-PW-220 RCVV lever arm pin (1992); Boeing 747-258F engine losses owing to a wing pylon failure (1992); Westland Lynx SH14D helicopter rotor hub (1998).

### 1.8.4 Virtual testing of non-generic aircraft components (M. Nawijn, NLR)

Virtual testing uses advanced simulation technology to support or partially replace physical tests. The main objectives are cost and risk reduction for actual tests needed in aircraft structural certification programmes. The structural levels addressed in virtual testing range from coupons at the lowest level to a full-scale component or aircraft at the highest level.

The NLR recently started a research programme in virtual testing. Both extremes of the structural levels found in aerospace structures are being addressed. At the coupon level the objective is to reduce the number of actual tests needed for material certification by developing models that accurately predict the fatigue and damage tolerance

characteristics of different composites (e.g. traditional laminates, woven fabrics, fibre tow-placement laminates). Reduction of the number of actual tests by virtual testing allows customers to economically introduce new combinations of composite materials and corresponding manufacturing processes.

### 1.8.5 Simulation of damage in composites (M. Nawijn, NLR)

There is a significant increase in the application of composite materials in primary aircraft structures. Studying the effects of damage under fatigue and static loading on the structural response and integrity of a component requires detailed knowledge of the physics governing damage mechanics and how to implement this knowledge in simulation codes.

The NLR has begun an extensive project to study damage in composites from both the physical and simulation perspectives. Different types of damage models are being investigated. On the smallest scale, theoretical micro-mechanical damage models are studied and verified by means of physical micro-coupon tests. The test results (data/images obtained from microscopy) are used to identify failure modes like matrix cracking, fibre/matrix debonding and fibre cracking. On a larger scale, more-empirical damage models are evaluated for applicability to different composite materials (e.g. woven fabric, stitched laminates) and manufacturing technologies like fibre tow-placement.

## 1.9 REFERENCES

- [1] Veul, R.P.G., Houwink, R., and Weert, J.F.H.W. van ; *Coupling and enhancement of existing spectra generation and fatigue and crack growth analysis tools*, NLR Contract Report NLR-CR-2008-756, National Aerospace Laboratory NLR, Amsterdam, the Netherlands.
- [2] Huls, R.A., and Veul, R.P.G.; *Design, implementation and validation of a fatigue critical area detector*, NLR Contract Report NLR-CR-2008-737, National Aerospace Laboratory NLR, Amsterdam, the Netherlands.
- [3] Wanhill, R.J.H., Platenkamp, D.J., Hattenberg, T., Bosch, A.F., and Haan, P.H. de; *GLARE teardowns from the MegaLiner Barrel (MLB) fatigue test*, NLR Technical Publication NLR-TP-2009-068, National Aerospace Laboratory NLR, Amsterdam, the Netherlands.
- [4] Schijve, J., Campoli, G., and Monaco, A.; *Fatigue of structures and secondary bending in structural elements*, International Journal of Fatigue, In press, Corrected proof online 2009.
- [5] Barter, S.A., and Wanhill, R.J.H.; *Marker loads for quantitative fractography of fatigue cracks in aerospace alloys*, NLR Technical Publication NLR-TP-2008-833, National Aerospace Laboratory NLR, Amsterdam, the Netherlands.
- [6] Tinga, T., Brekelmans, W.A.M., and Geers, M.G.D.; *Time-incremental creep-fatigue damage rule for single crystal Ni-base superalloys*, Materials Science and Engineering A, In press, Corrected proof online 2009.
- [7] Wanhill, R.J.H.; *Some notable aircraft service failures investigated by the National Aerospace Laboratory NLR*, Structural Integrity and Life, In press 2009. Also: NLR Technical Publication NLR-TP-2009-001, National Aerospace Laboratory NLR, Amsterdam, the Netherlands.

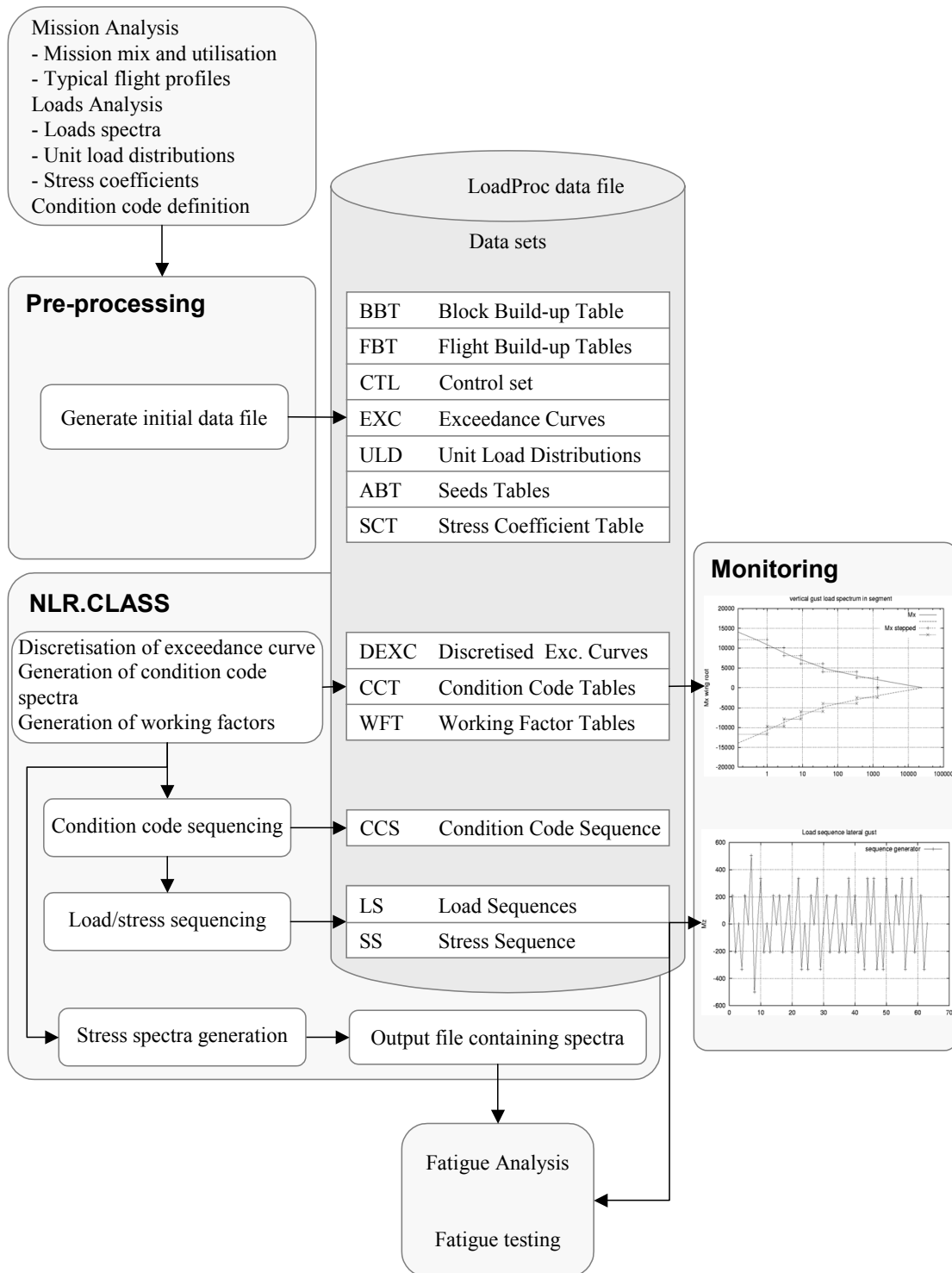


Fig. 1 Flow diagram of the CLASS programme for generation of sequences for loads or stresses for aircraft structures

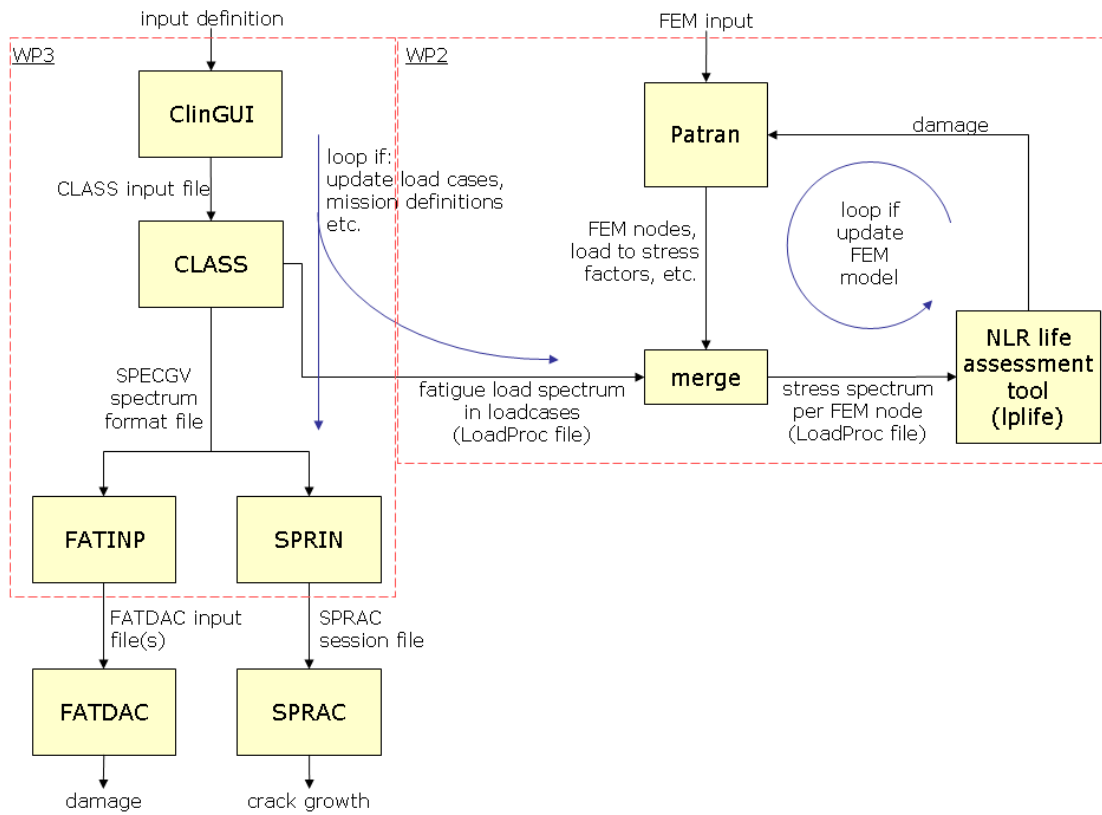


Fig. 2 Relations between the various tools coupled with CLASS

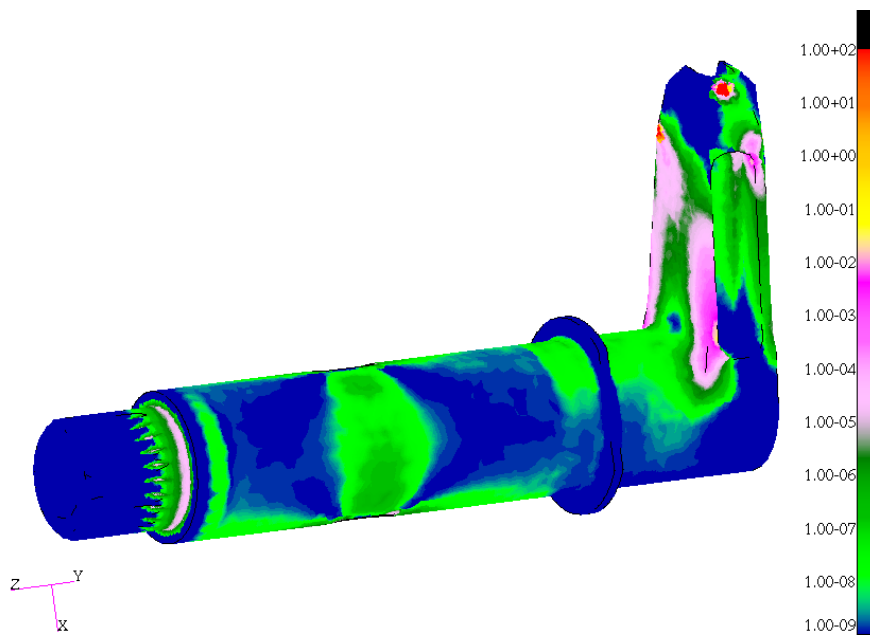


Fig. 3 Detection of fatigue-critical areas (red) in a hinge from a sliding door in a pressure cabin



Fig. 4 Use of the fatigue life monitoring system HOLMES

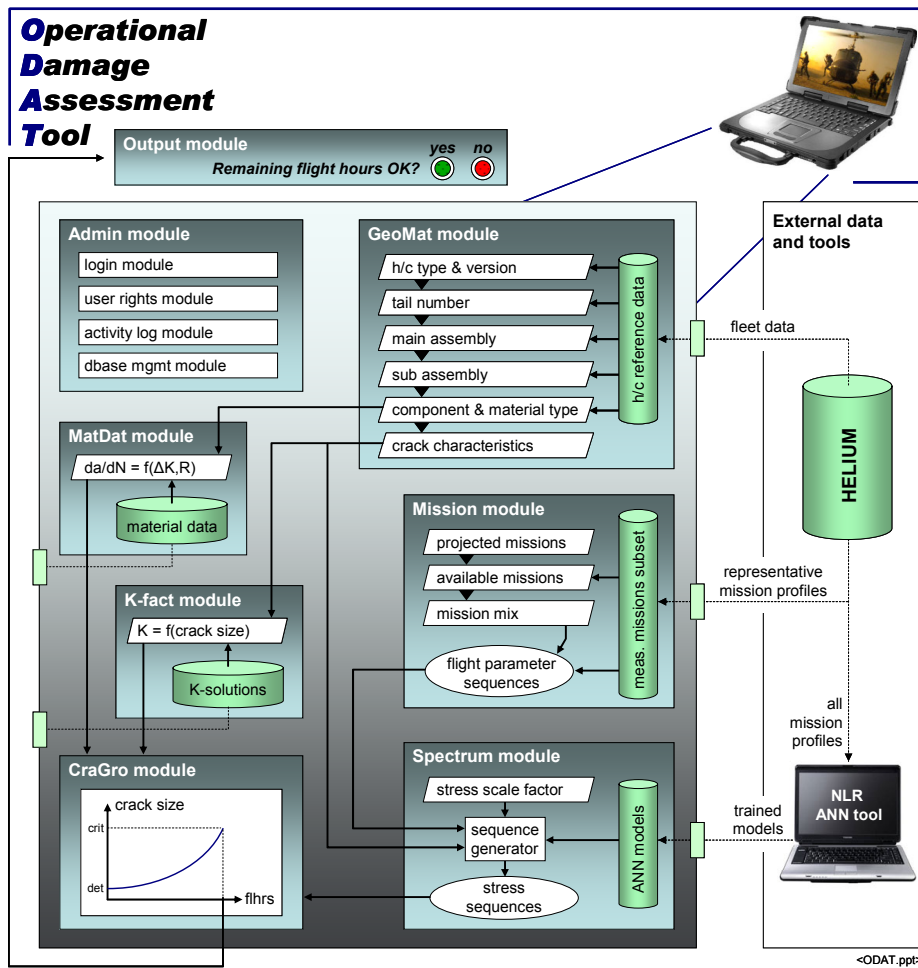


Fig. 5 The ODAT system architecture for HeliDamTol



Fig. 6 NH90 NATO Frigate Helicopter version acquired by the RNLN

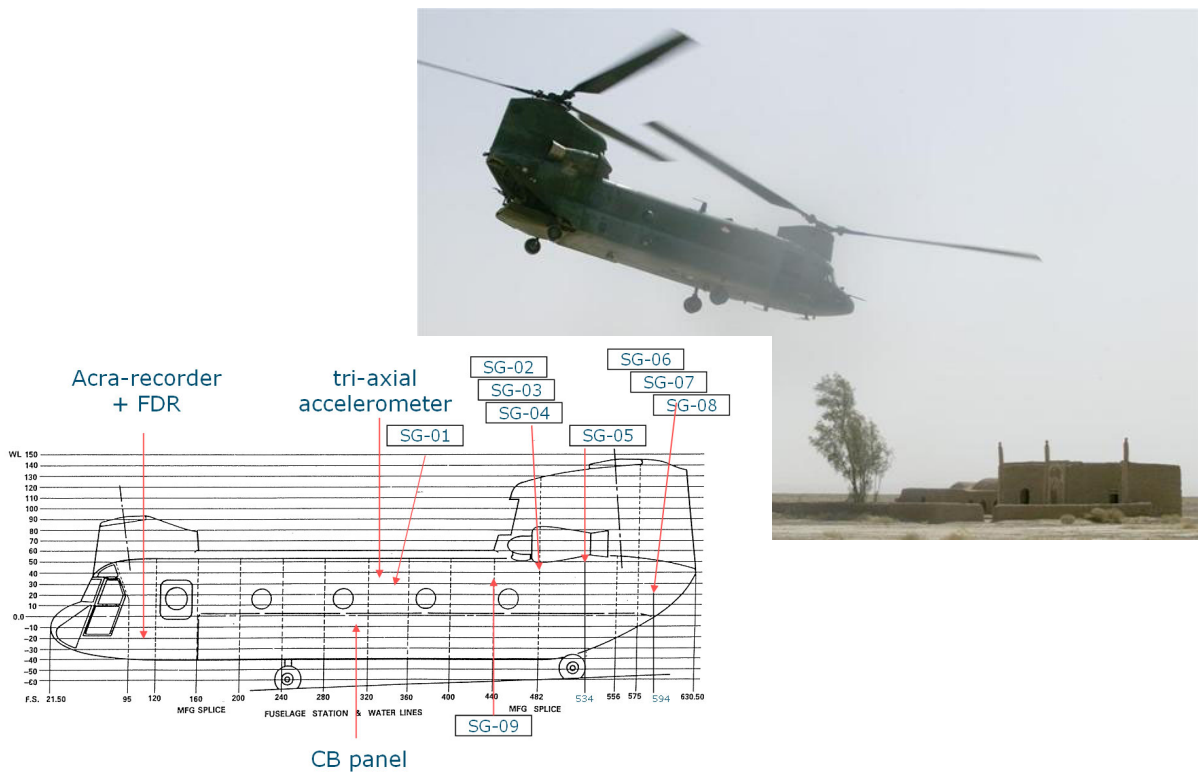


Fig. 7 ACRA data acquisition unit and strain gauge (SG) locations in Chinook helicopters



Fig. 8 Salsa applications



Fig. 9 AHMOS key system components installed in a pod on a Hawk aircraft for flight testing in the UK

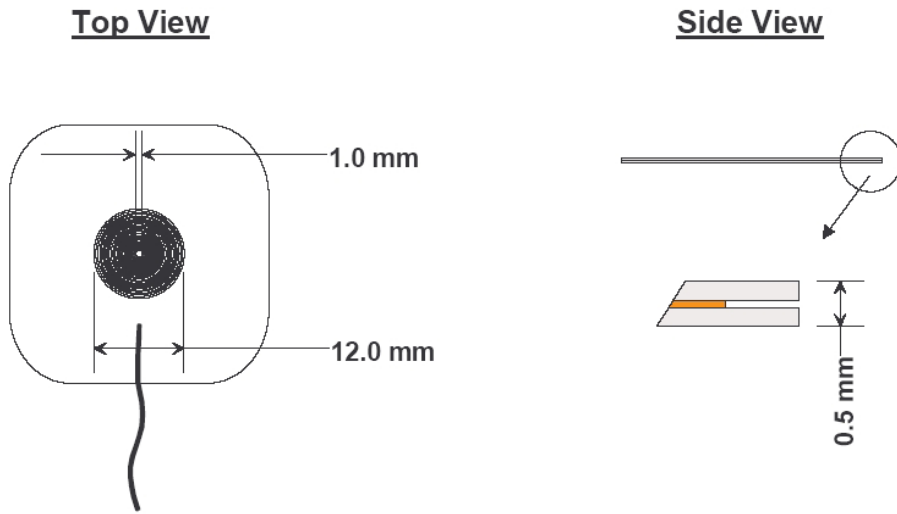


Fig. 10 Flexible absolute sensor for high-frequency surface crack detection in a radius area. Centre frequency 800 kHz

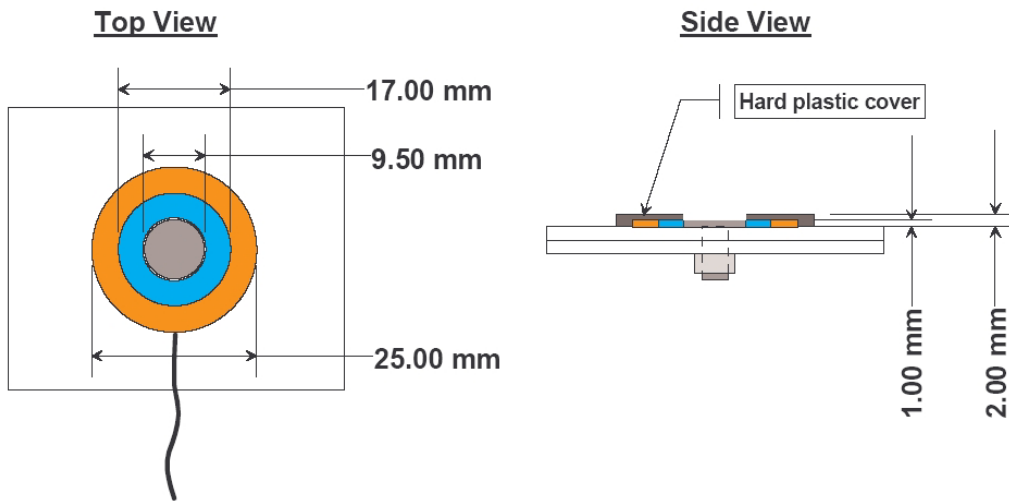


Fig. 11 Rigid reflection ring sensor for low-frequency crack detection around fasteners. Outside generator and internal receiver. Centre frequency 5 kHz

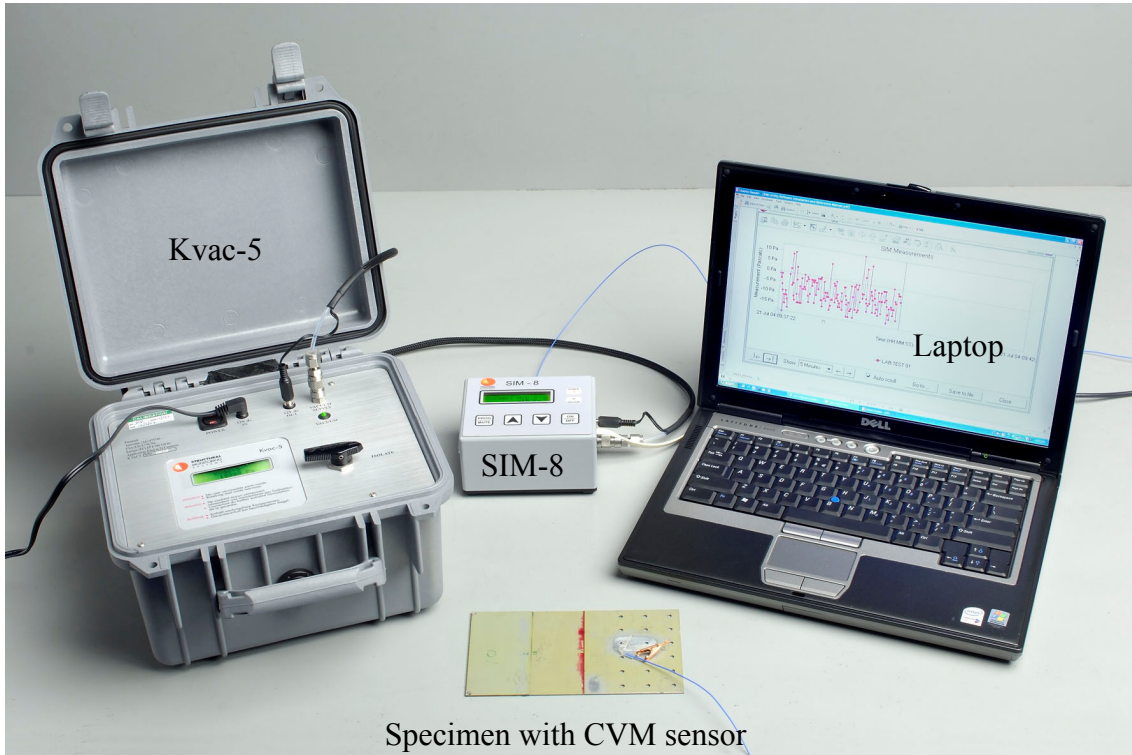


Fig. 12 Main components of the comparative vacuum monitoring (CVM) system. A stable reference vacuum source (Kvac-5), a highly sensitive flow meter (SIM-8), a laptop for data logging and a specimen with CVM sensor

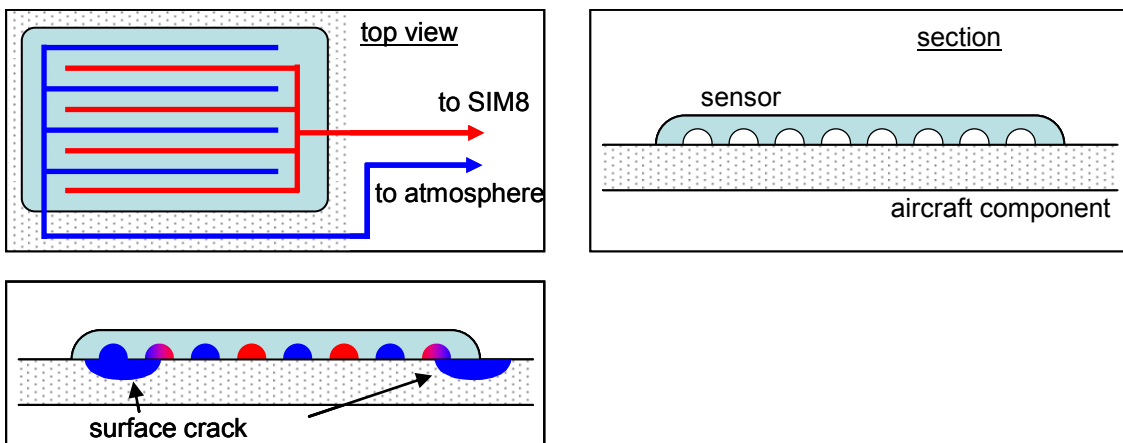


Fig. 13 Comparative vacuum monitoring (CVM) technique. The red lines represent the vacuum galleries, the blue lines the atmospheric galleries of the sensor

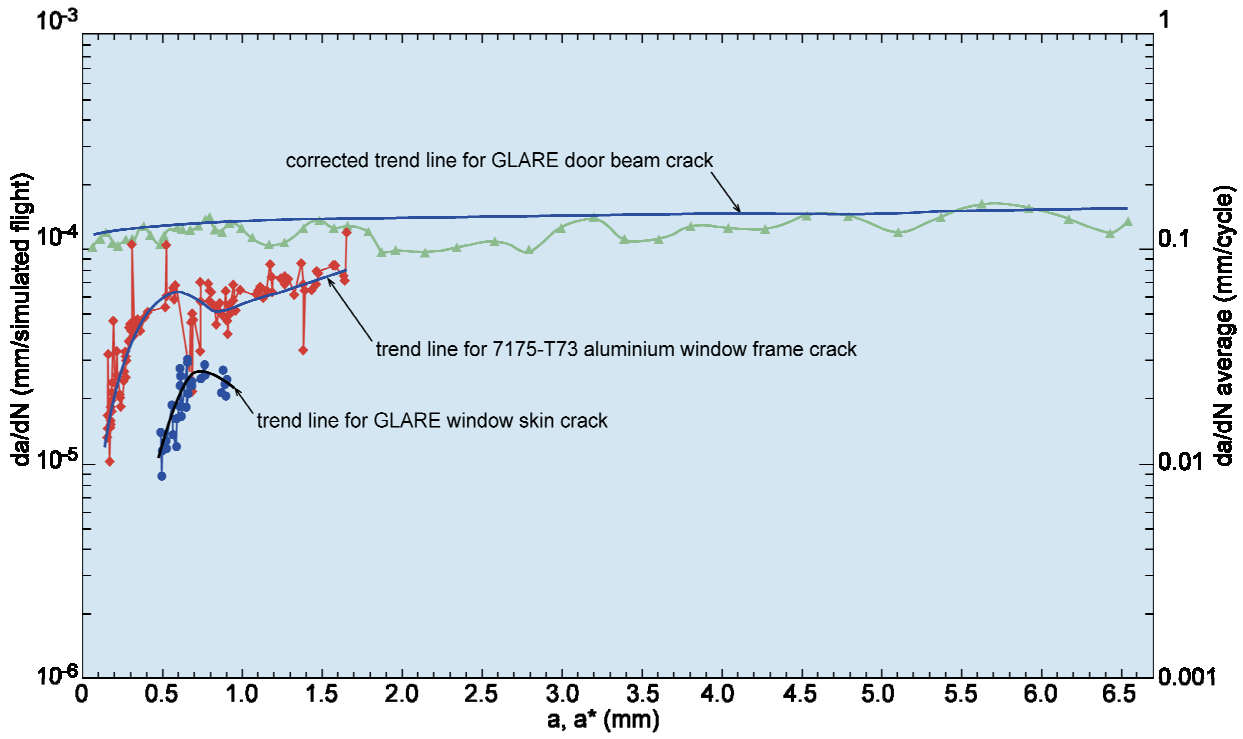


Fig. 14 Crack growth rates for the longest fatigue cracks in the door beam and window locations of the MegaLiner Barrel (MLB) [3]

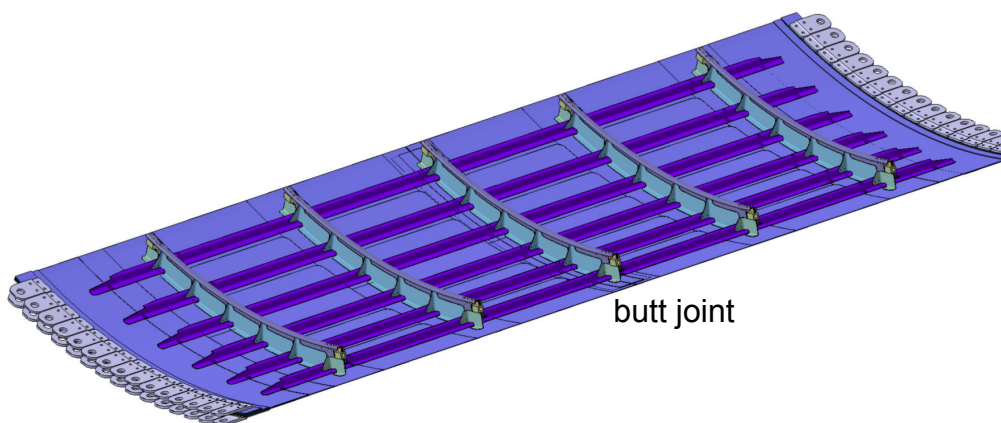


Fig. 15 Model of the curved GLARE fuselage panel

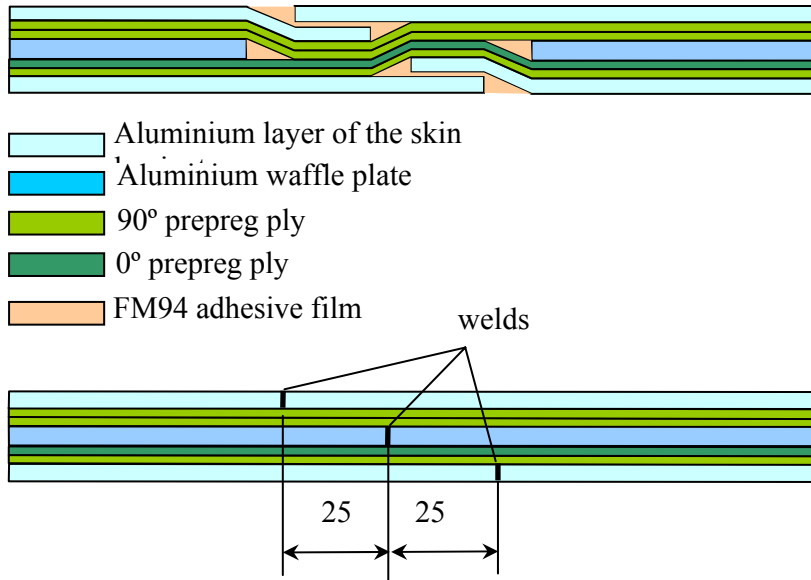
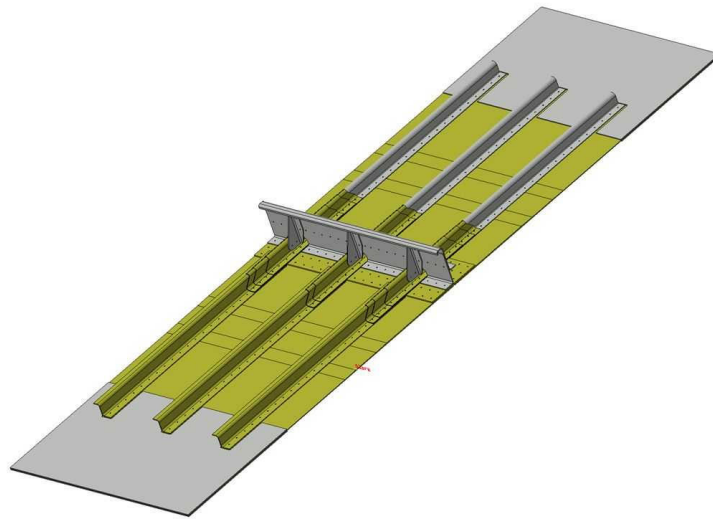


Fig. 16 Schematic cross-sections of standard bonded splice and friction stir weld (FSW) underneath the frames of the curved GLARE fuselage panel



Fig. 17 The NLR fuselage panel test rig

1/27



*Fig.18 Model of the GLARE stringer coupling panel*



*Fig. 19 GLARE stringer coupling panel during testing at the NLR*



Fig. 20 Failure of the GLARE stringer coupling panel in the stringer runout area

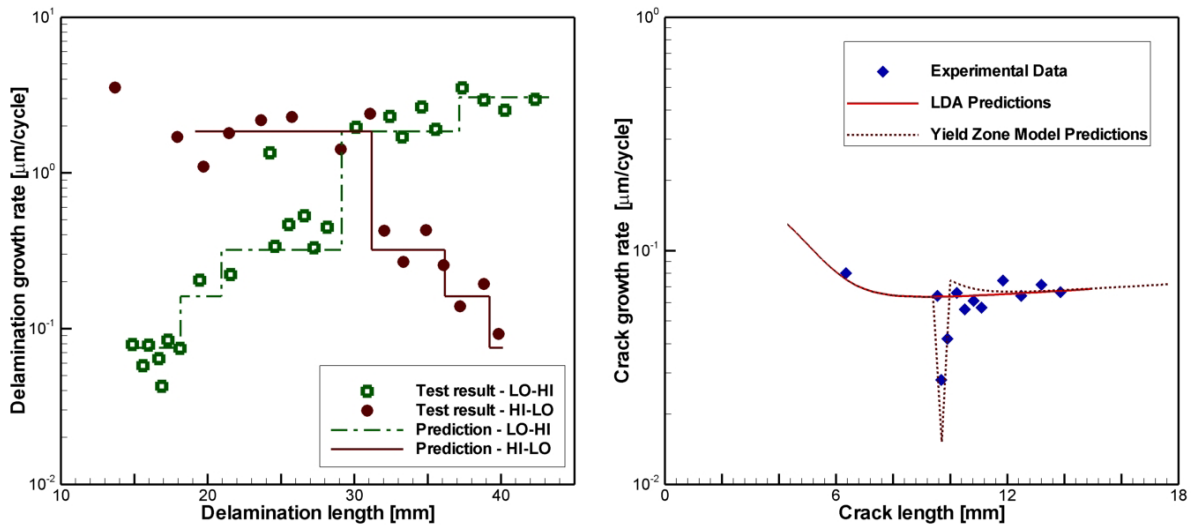


Fig. 21 (I) Measured delamination growth under multiple block loading  
 (II) Experimental and predicted crack growth before and after a single overload in a constant amplitude baseline test: predictions using a linear damage accumulation (LDA) model and a yield zone model.

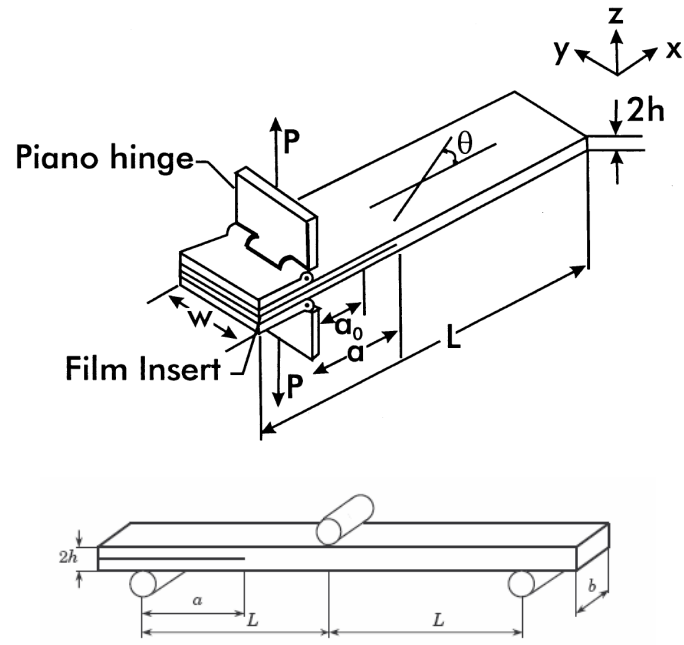


Fig. 22 The mode I DCB specimen (upper) and the mode II ENF (lower) specimen configurations

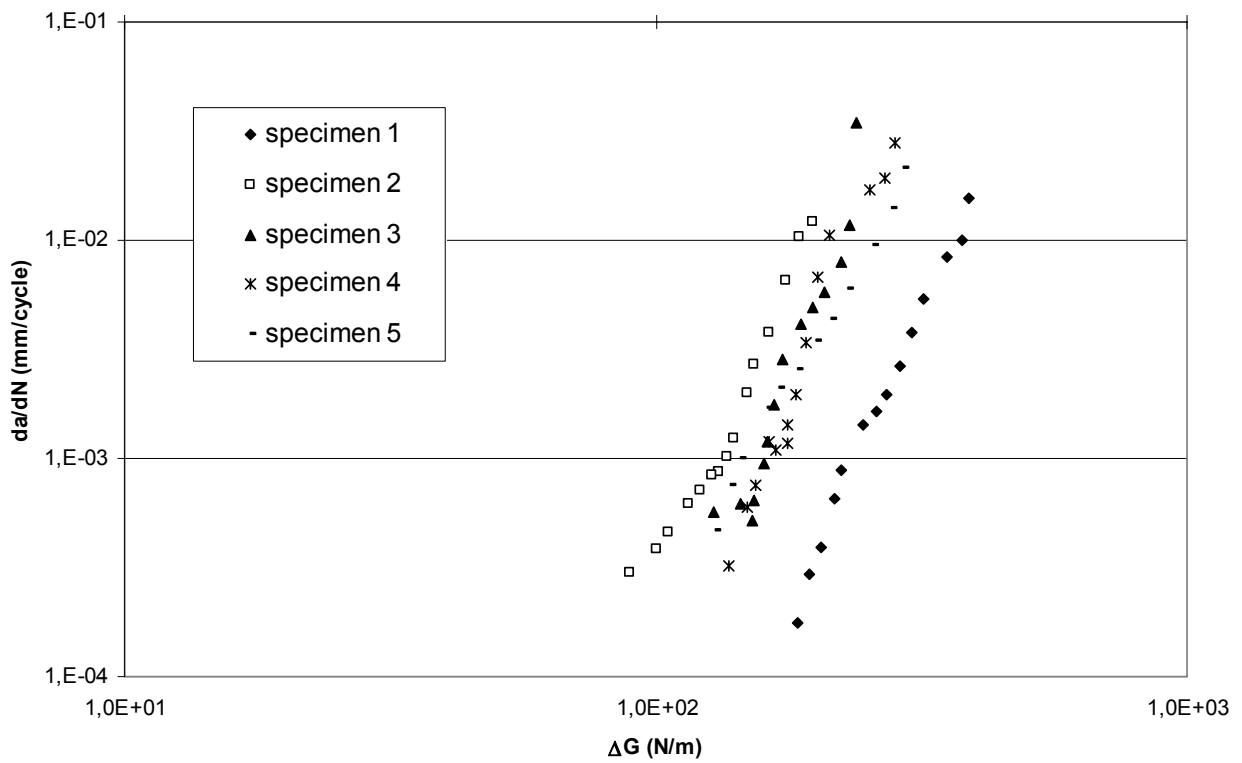


Fig. 23 Paris-type relation between delamination growth rate and maximum strain energy release rate for DCB specimens tested under mode I loading

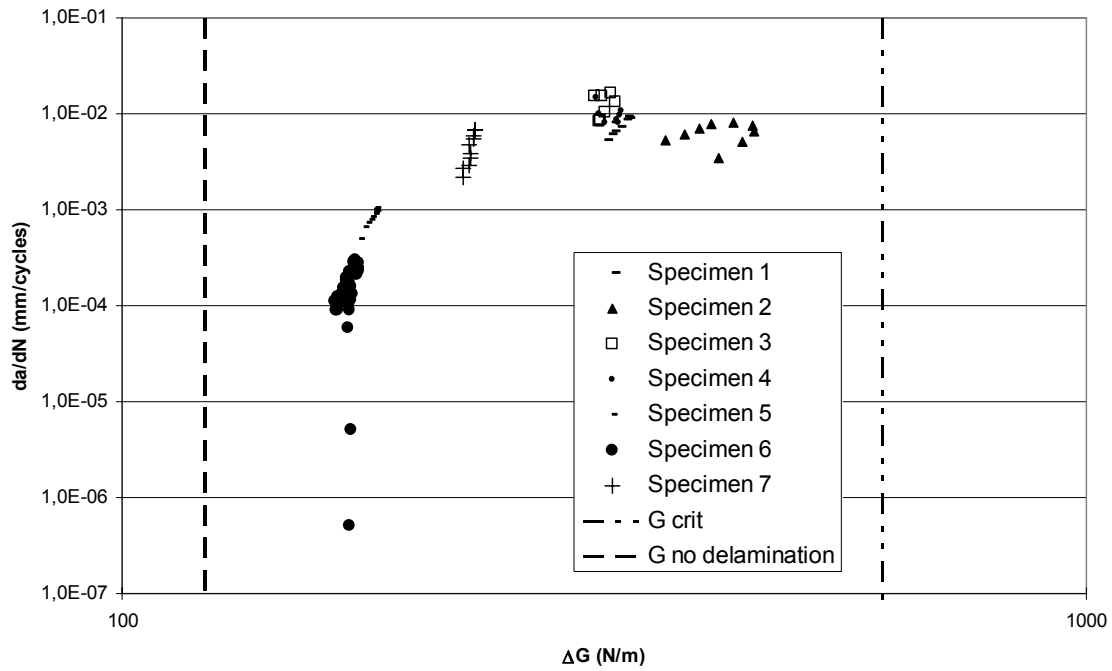


Fig. 24 Relation between delamination growth rate and strain energy release rate for ENF specimens tested under mode II loading

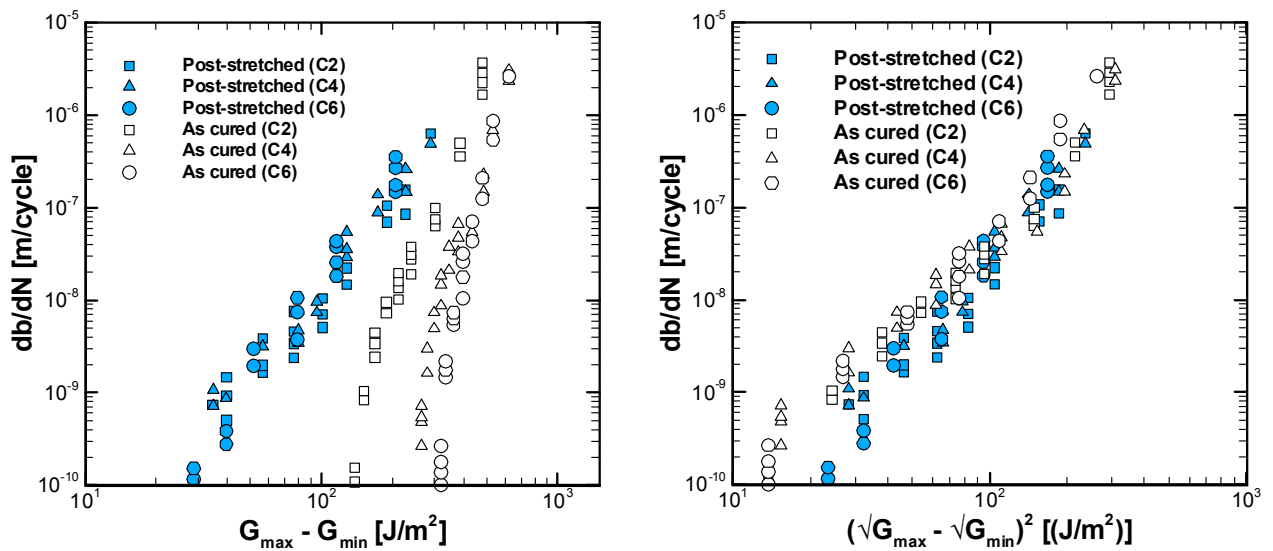


Fig. 25 Improved correlation of mode II delamination growth behaviour (right-hand diagram) for carbon fibre/aluminium laminates with varying number of carbon fibre layers (C#) in the as-cured (with residual stress) and post- stretched (no residual stress) conditions

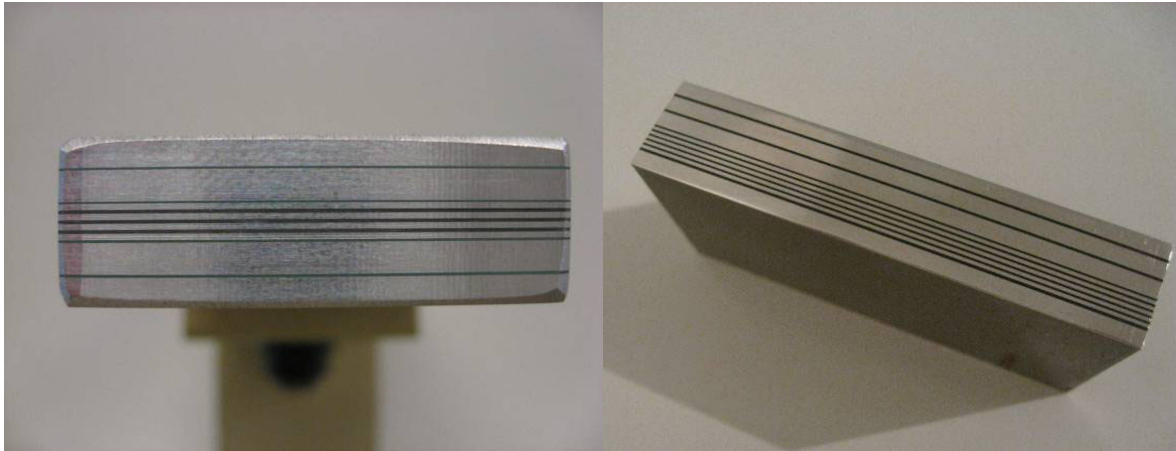


Fig. 26 Two examples of CentraI: a laminate with central GLARE core and four 2 mm thick aluminium sheets bonded with adhesive (left) and a laminate with GLARE core and four aluminium sheets bonded with Bondpreg in an asymmetric configuration (right)

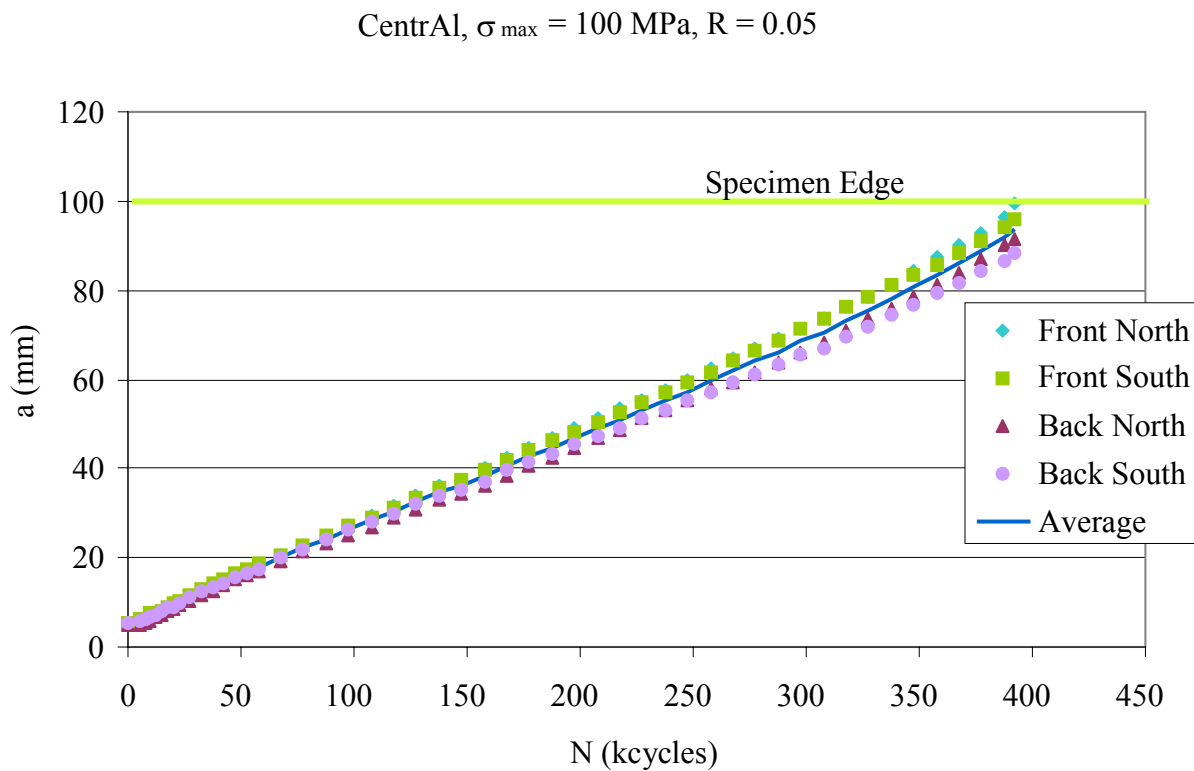


Fig. 27 Constant amplitude fatigue crack growth curve for the outer aluminium sheets during a CentraI test. The crack growth rates are nearly constant throughout the life of the specimen

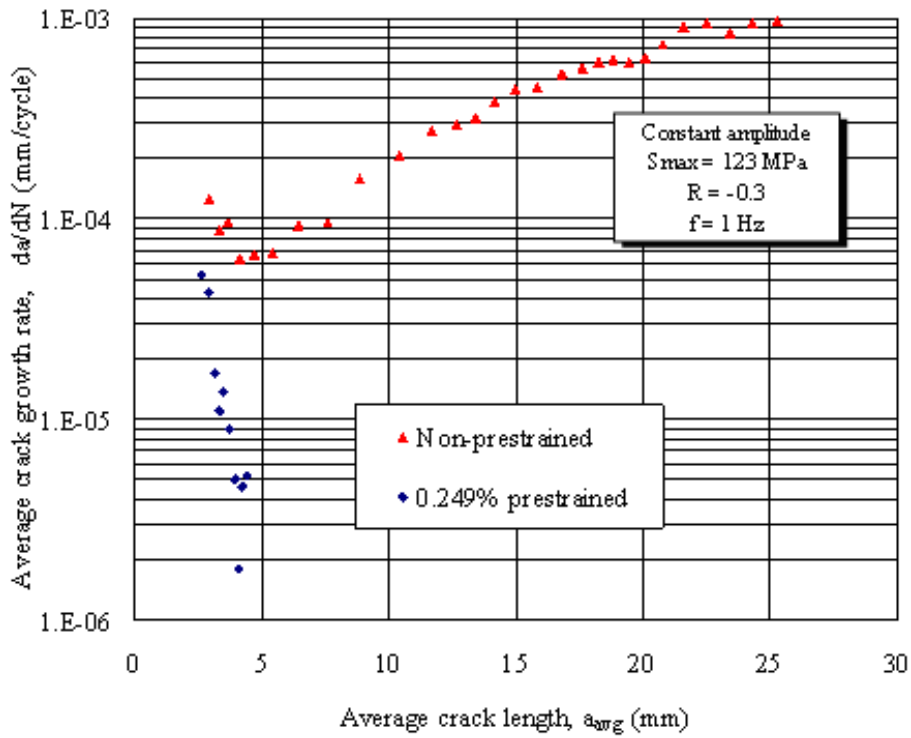


Fig. 28 Effect of prestraining on fatigue crack growth in Zylon FML 2-3/2-0.3 laminates

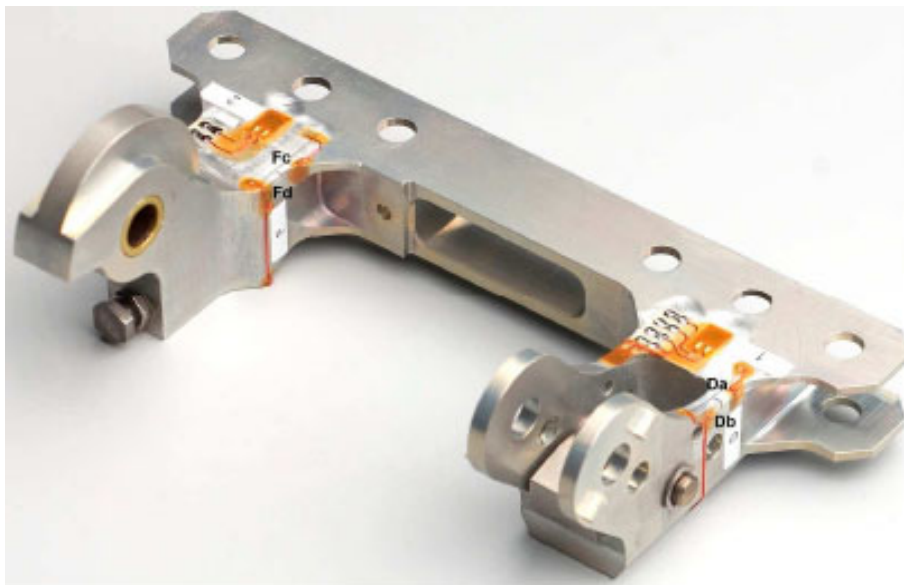


Fig. 29 ATV panel hinge with crack starter notches  $D_a$ - $D_b$  and  $F_c$ - $F_d$  and 5 bonded-on strain gauges



*Fig. 30 ATV panel hinge specimen (at top of picture) in the ad hoc test rig*

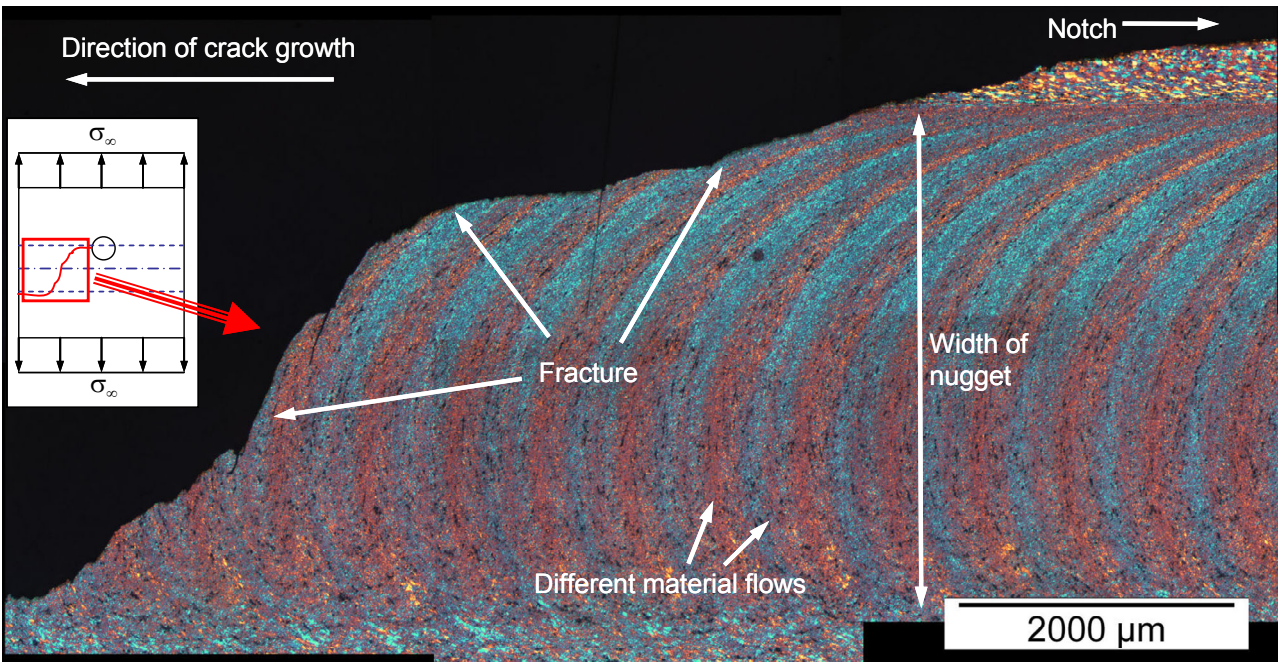


Fig. 31 FSW microstructure and fatigue crack path change across the weld bead (nugget). The inset shows the overall crack path

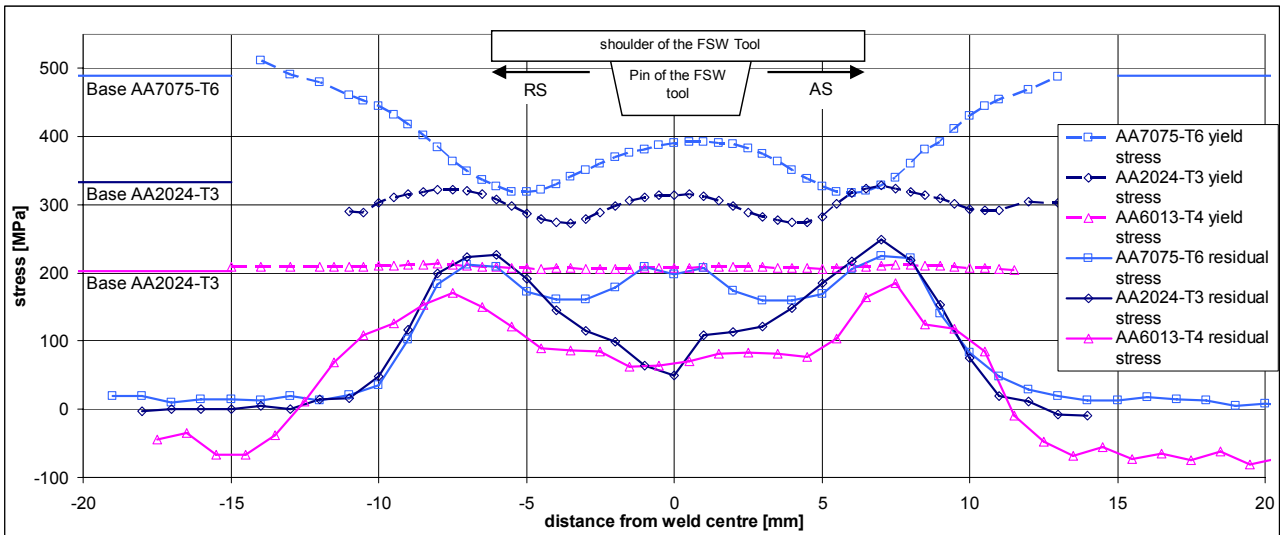


Fig. 32 Residual stress profiles and local yield strengths for FSW Al 2024-T3, Al 7075-T6 and Al 6013-T4

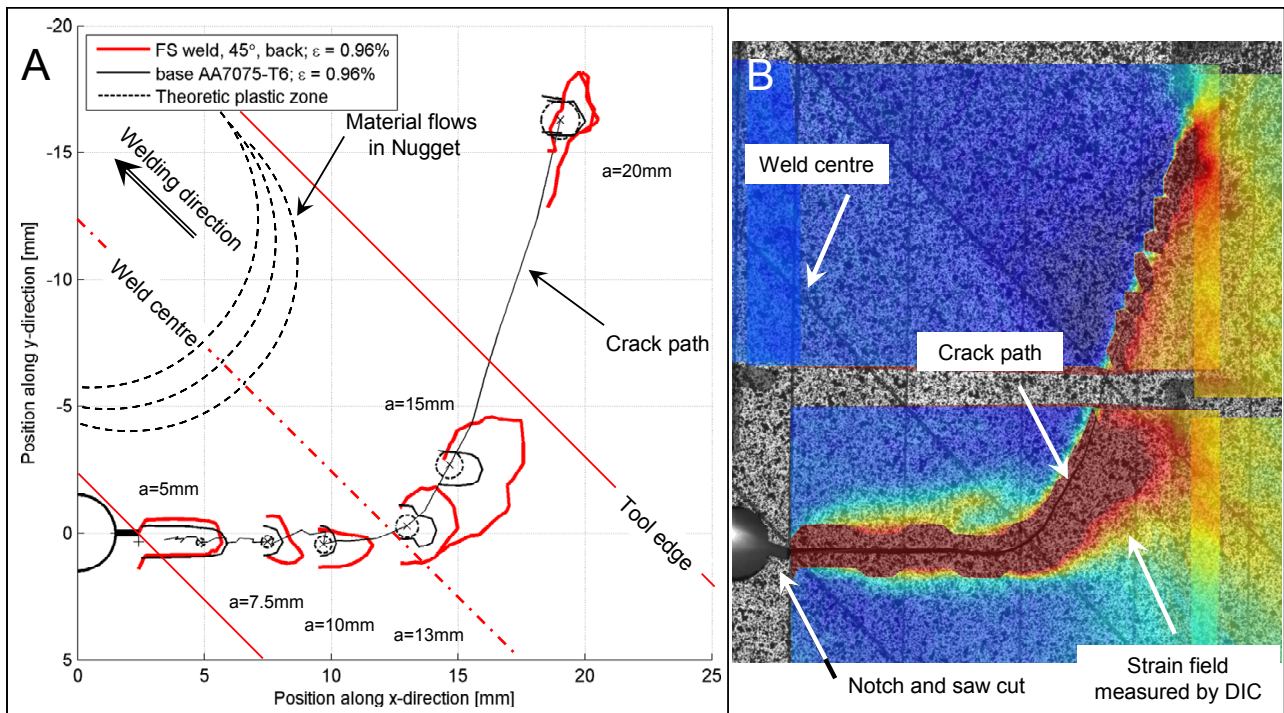


Fig. 33 (A) Contour plot of plastic zone for different fatigue crack lengths in FSW Al 7075-T6; (B) DIC-measured strain field around the crack

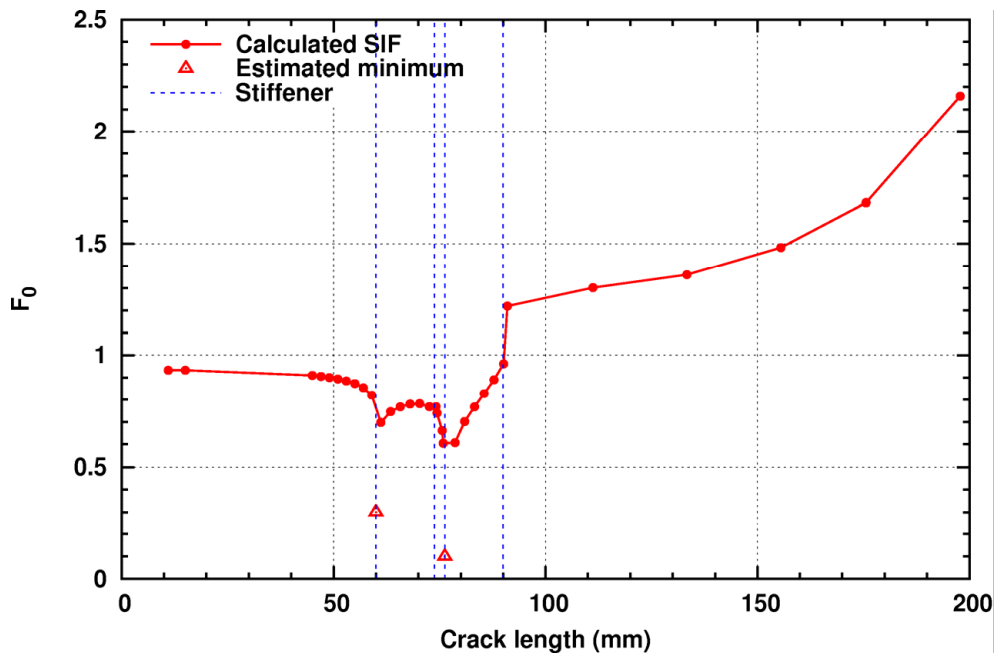


Fig. 34 Predicted normalised stress intensity factor (SIF) for a DaToN panel with two stiffeners (one T-stiffener indicated in the diagram) and a central crack growing towards the stiffener.

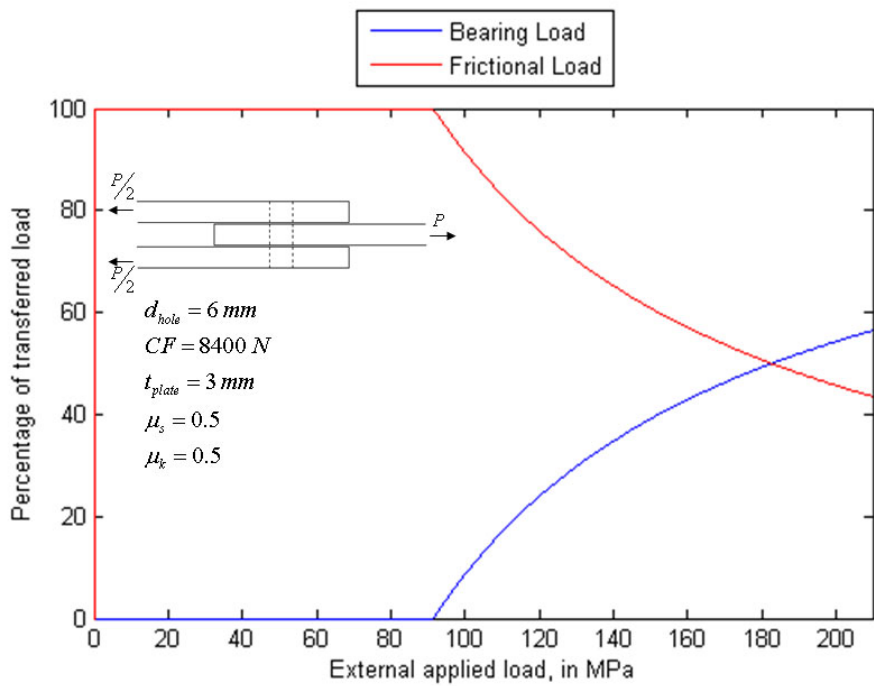


Fig. 35 Example prediction of the splitting of frictional and bearing load transfer in a single-row double-shear bolted joint

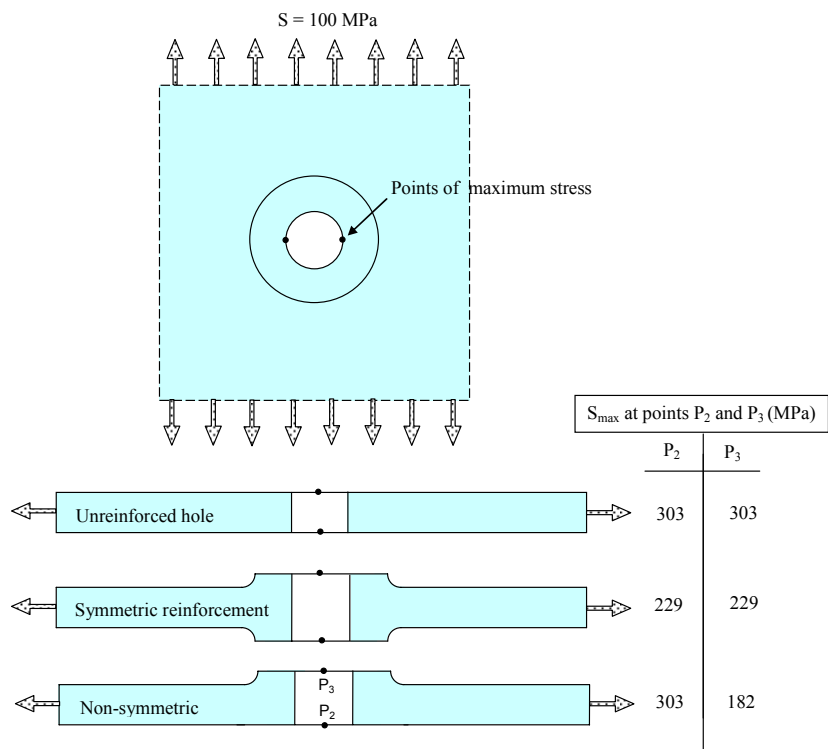


Fig. 36 Effect of symmetric and non-symmetric hole edge reinforcements on the peak stress at the edge of the hole (FE results)

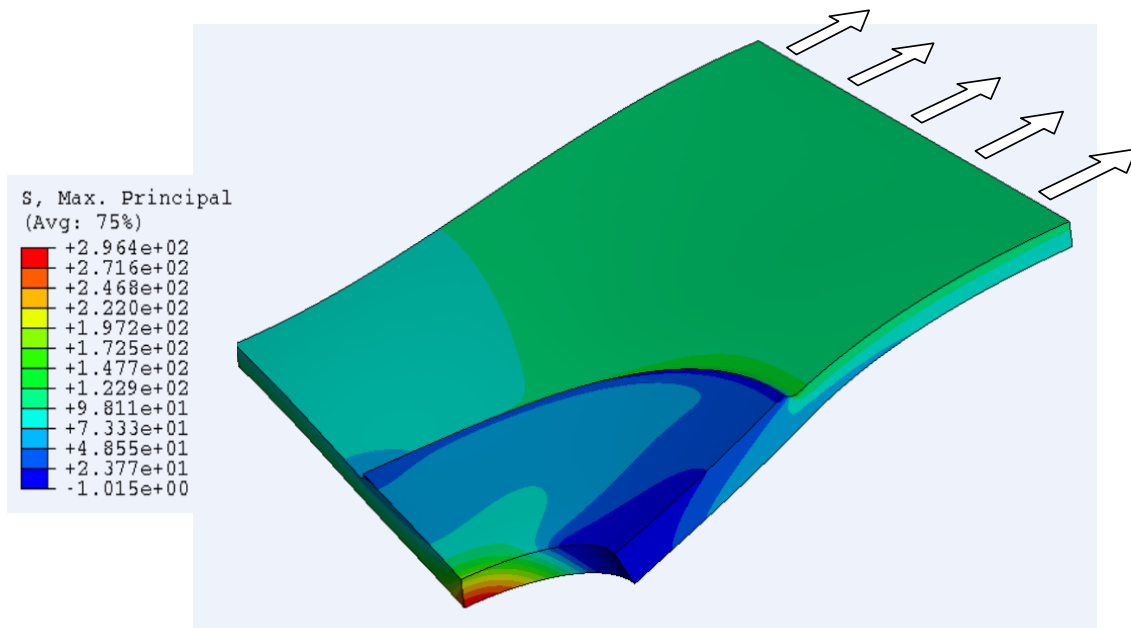


Fig. 37 Out-of-plane displacements and stress distribution for the non-symmetric hole edge reinforcement shown in figure 36

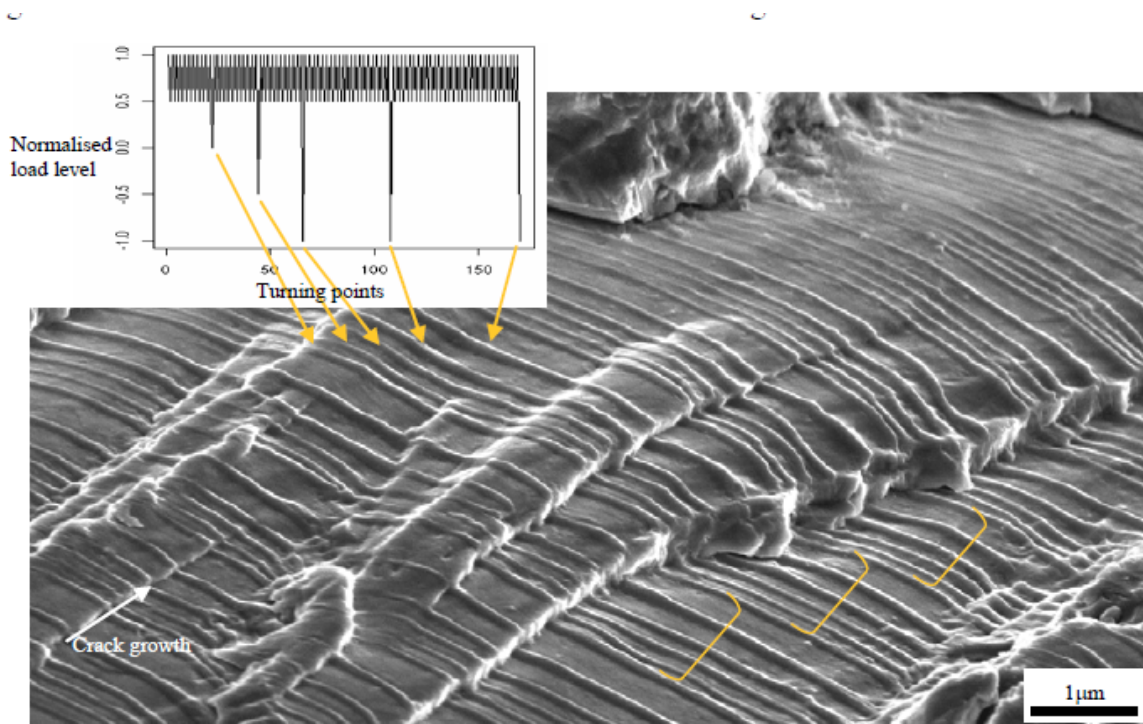
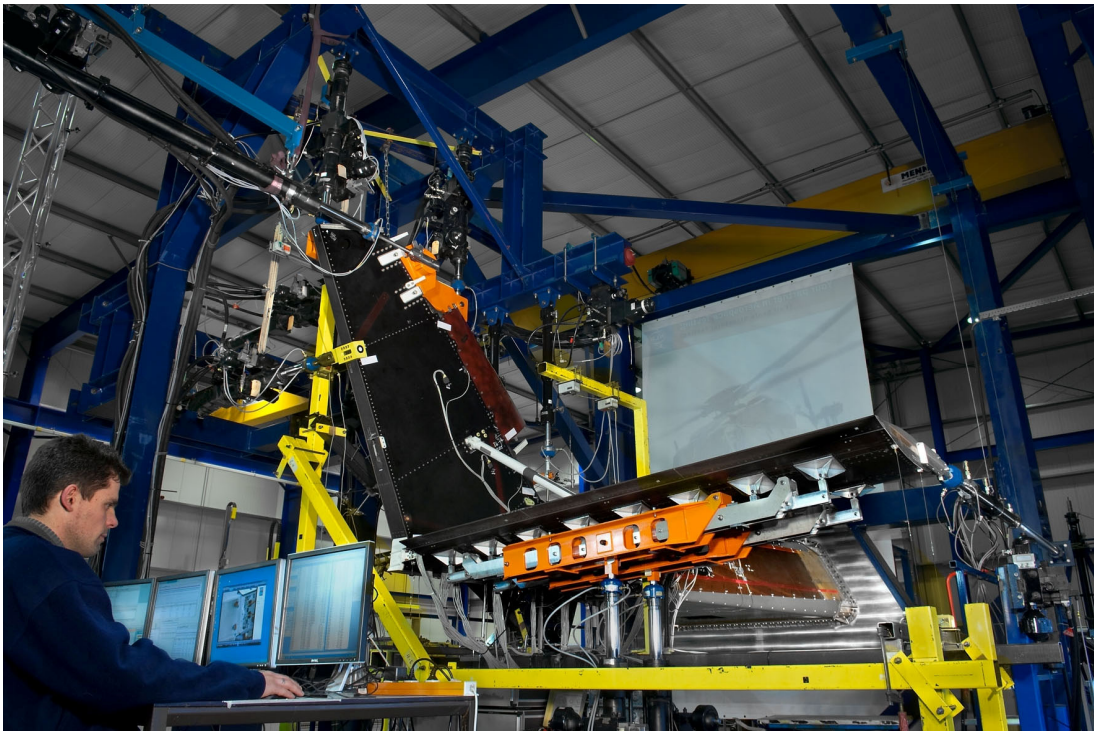


Fig.38 Scanning Electron Microscope (SEM) fractograph of repeat underloads on the fatigue fracture surface of an Al 7050-T7451 specimen. The underloads produced well-defined markers that allowed each underload to be identified



*Fig. 39 Composite lug details for proof of concept evaluation of a generic composite brace*



*Fig. 40 NH90 tail module full-scale test set-up*

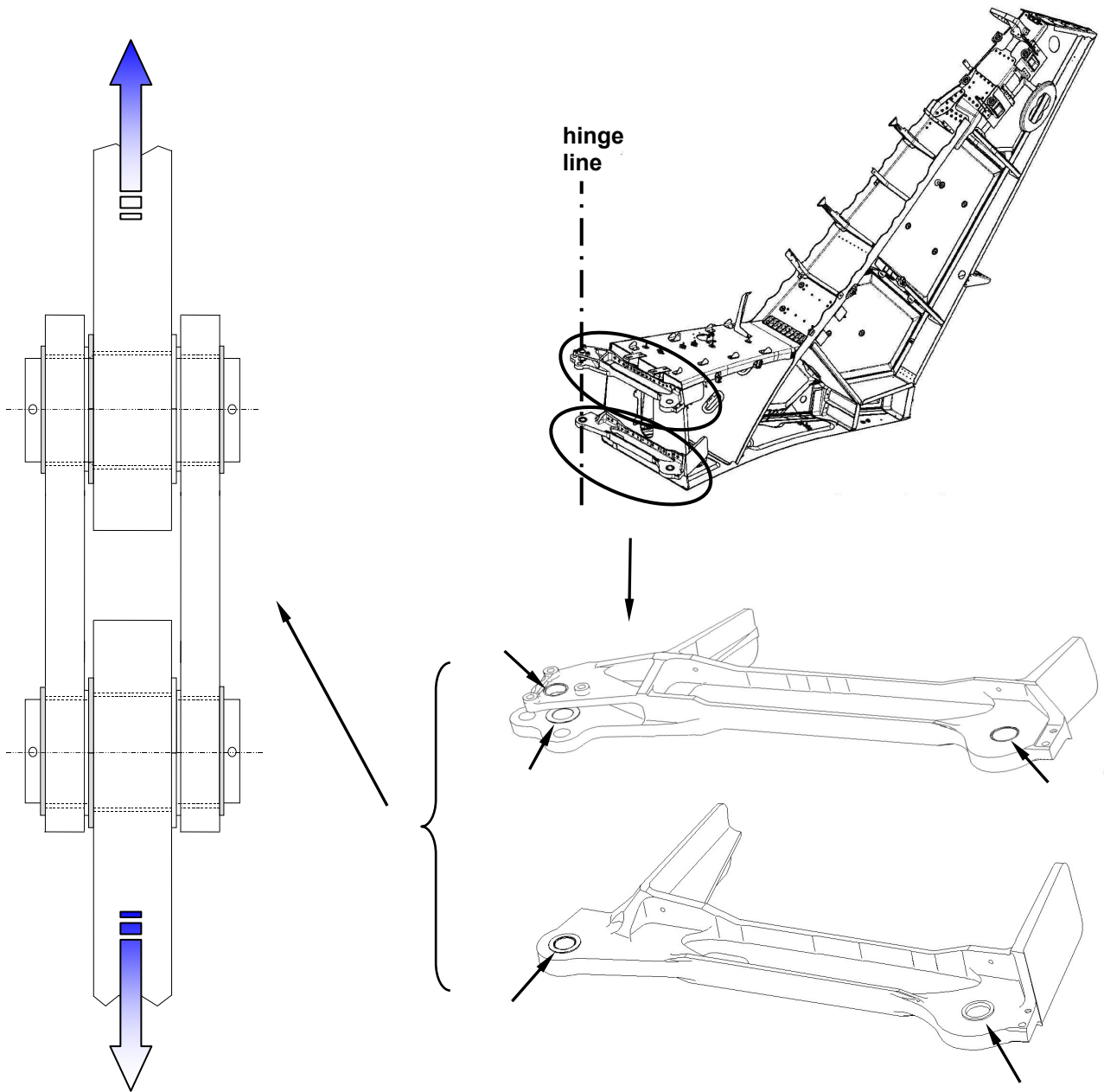


Fig. 41 NH90 helicopter tail hinge lugs with indications of flaw tolerance locations